MASTERARBEIT | MASTER'S THESIS

Titel | Title

Adsorptive preservation of DNA on goethite under the influence of competing species

verfasst von | submitted by

Paul Johann Klier BSc

angestrebter akademischer Grad | in partial fulfilment of the requirements for the degree of

Master of Science (MSc)

Wien | Vienna, 2026

Studienkennzahl lt. Studienblatt | Degree programme code as it appears on the student record sheet:	UA 066 815
Studienrichtung lt. Studienblatt | Degree programme as it appears on the student record sheet:	Masterstudium Erdwissenschaften
Betreut von | Supervisor:	Univ.-Prof. Dipl.-Geol. Dr. Stephan Krämer

Acknowledgements

I gratefully acknowledge the support and guidance of all those who contributed to this thesis. My sincere thanks go to Stephan Krämer for giving me the opportunity to work on this topic and for his constructive feedback and valuable discussions throughout the course of this project. Special thanks go to Veer Singh, who was always available for subject-specific, laboratory-related and general project-related questions. I would also like to thank Anita Brijit for her guidance and mentorship in the laboratory as well as for her support during the writing process. Finally, I would like to thank the entire EDGE working group for their support, especially Herwig Lenitz and Jiahui Wu.

Abstract

Environmental DNA (eDNA) preserved in soil and sediments is a critical genetic archive for paleoenvironmental reconstruction, biodiversity monitoring and plays a crucial role in biogeochemical processes such as phosphorus cycling and horizontal gene transfer. While non-bound extracellular DNA in solution degrades rapidly, primarily through microbial nuclease activity, DNA can persist for up to 2 million years in sediments. This exceptional long-term preservation is widely attributed to adsorption onto mineral surfaces, which reduces susceptibility to enzymatic decay. However, mineral surfaces in natural environments are rarely pristine and are typically coated with organic and inorganic molecules that may compete for surface binding sites, thereby potentially altering DNA adsorption dynamics and long-term preservation. Despite this complexity, most previous studies have relied on pristine mineral surfaces and have largely overlooked the effects of competing species. Here, it was investigated how model organic and inorganic competitors, bovine serum albumin (BSA) and phosphate, affect the adsorption, desorption and protection from enzymatic hydrolysis of DNA fragments of varying lengths, 99, 1000, and ~20,000 base pairs (bp), on a model Fe(III)-oxyhydroxide, goethite. Results show that both competitors significantly reduced DNA adsorption, with phosphate exerting a stronger inhibitory effect than BSA. Desorption increased with decreasing polymer length due to the ease of desorption of fewer surface attachment points. Sequential versus simultaneous addition experiments show that the system did not reach equilibrium within three weeks, indicating kinetically controlled adsorption–desorption processes. Additionally, the comparatively slow desorption and a “non-desorbable” fraction of DNA indicates kinetical trapping. Hydrolysis using a model endonuclease, DNase I, reveals an enhanced enzymatic degradation in the presence of BSA or phosphate relative to pristine goethite, although short fragments embedded within BSA multilayers exhibited partial physical protection. Together, these findings demonstrate that competing species substantially reduce DNA adsorption, promote desorption and increase susceptibility to enzymatic decay.

Kurzfassung

Umwelt-DNA (eDNA), die in Böden und Sedimenten konserviert ist, stellt ein wichtiges genetisches Archiv für die Rekonstruktion früherer Umweltbedingungen und Biodiversitätsmonitoring dar und spielt zudem eine zentrale Rolle in biogeochemischen Prozessen wie dem Phosphorkreislauf und dem horizontalen Gentransfer. Während nicht gebundene extrazelluläre DNA in Lösung hauptsächlich durch mikrobielle Nukleaseaktivität rasch abgebaut wird, kann DNA in Sedimenten bis zu 2 Millionen Jahre überdauern. Diese außergewöhnlich lange Konservierung wird weithin der Adsorption an Mineraloberflächen zugeschrieben, wodurch die Anfälligkeit für enzymatischen Abbau verringert wird.

Mineraloberflächen in natürlichen Umgebungen sind jedoch selten rein, sondern typischerweise mit organischen und anorganischen Molekülen bedeckt, die um Bindungsstellen konkurrieren und dadurch die Adsorptionsdynamik von DNA sowie ihre langfristige Erhaltung beeinflussen können. Trotz dieser Komplexität basieren die meisten bisherigen Studien auf reinen Mineraloberflächen und berücksichtigen konkurrierende Spezies nur unzureichend. In dieser Arbeit wird untersucht, wie Modell-Konkurrenten organischer und anorganischer Natur, Rinderserumalbumin (BSA) und Phosphat, die Adsorption, Desorption und den Schutz vor enzymatischer Hydrolyse von DNA-Fragmenten unterschiedlicher Länge (99, 1000 und ~20.000 Basenpaare) an einem Modell-Fe(III)-Oxyhydroxid, Goethit, beeinflussen. Die Ergebnisse zeigen, dass beide Konkurrenten die DNA-Adsorption deutlich reduzieren, wobei Phosphat einen stärkeren hemmenden Effekt ausübt als BSA. Die Desorption nimmt mit abnehmender Polymerlänge zu, da kürzere Moleküle über weniger Oberflächenkontaktpunkte verfügen und daher leichter gelöst werden. Experimente mit sequenzieller versus simultaner Zugabe zeigen, dass das System innerhalb von drei Wochen kein Gleichgewicht erreicht, was auf kinetisch kontrollierte Adsorptions-Desorptionsprozesse hinweist. Zusätzlich deuten die vergleichsweise langsame Desorption und ein „nicht desorbierbarer“ Anteil von DNA auf kinetische Trapping-Effekte hin. Experimente zur Hydrolyse mittels der Modell-Endonuklease DNase I zeigen eine verstärkte enzymatische Degradation in Anwesenheit von BSA oder Phosphat im Vergleich zu reinem Goethit, wobei kurze Fragmente, die in BSA-Multischichten eingebettet sind, teilweise physikalisch geschützt wurden. Insgesamt zeigen die Ergebnisse, dass konkurrierende Spezies die DNA-Adsorption deutlich verringern, die Desorption fördern und die Anfälligkeit gegenüber enzymatischem Abbau erhöhen.

Table of Contents

List of Figures:

List of Tables:

1. Introduction

Advances in the analysis of deoxyribonucleic acid (DNA) derived from environmental samples, such as soil, sediments, water, ice, etc. commonly referred to as environmental DNA (eDNA), have enabled a wide range of applications. These include the analysis of the genetic information stored in eDNA for biodiversity monitoring (Thomsen and Willerslev 2015) and spatial species distribution (Vasar et al. 2023; Borràs Sayas et al. 2025). eDNA has also been used in paleoenvironmental reconstruction of terrestrial and marine ecosystems ranging up to 2 million years old (Kjær et al. 2022). Beyond ecological relevance, eDNA is also used in forensic science (Allwood et al. 2020) and human disease monitoring (Whitmore et al. 2023). A comprehensive understanding of the fate of eDNA in environmental systems is critical not only for advancing methodological developments in environmental sciences but also because eDNA plays a crucial role in biogeochemical processes like nutrient cycling (Dell'Anno und Corinaldesi 2004; Ye et al. 2022) and horizontal gene transfer (Sand und Jelavić 2018). Moreover, the effectiveness of DNA-based technologies and the ecological significance of eDNA in biogeochemical processes depend strongly on its quality, stability and bioavailability. This underscores the importance of elucidating the geochemical factors that govern the persistence and transformation of DNA in environmental matrices.

1.1 DNA structure: A polyelectrolyte model

DNA is a biopolymer composed of two complementary nucleotide chains that form a double-helical structure. Each nucleotide is composed of one of the four nucleobases (adenine (A), thymine (T), cytosine (C), guanine (G)), a deoxyribose sugar and a phosphate group (Fig. 1). In each nucleotide, the nucleobase is attached to the deoxyribose sugar at the C1’ position, while the phosphate group links the sugars at the C3’ and C5’ positions to form the sugar–phosphate backbone (Fig. 1) (Frank-Kamenetskii 1997; Pray 2008).

The two complementary, antiparallel strands of DNA polymers are held together by hydrogen bonds (or H-bonds), where A binds with T with a double H-bond and G binds with C via a triple H-bond. With increasing temperature, the H-bonds holding the complementary DNA strands together start getting disrupted, resulting in single stranded DNA and the process is called DNA melting. The temperature at which half of the overall DNA molecules convert into single stranded DNA is termed melting temperature. The double stranded DNA exists in three primary conformations, right-handed helices, like A- and B-DNA or left-handed as in Z-DNA. (Frank-Kamenetskii 1997)

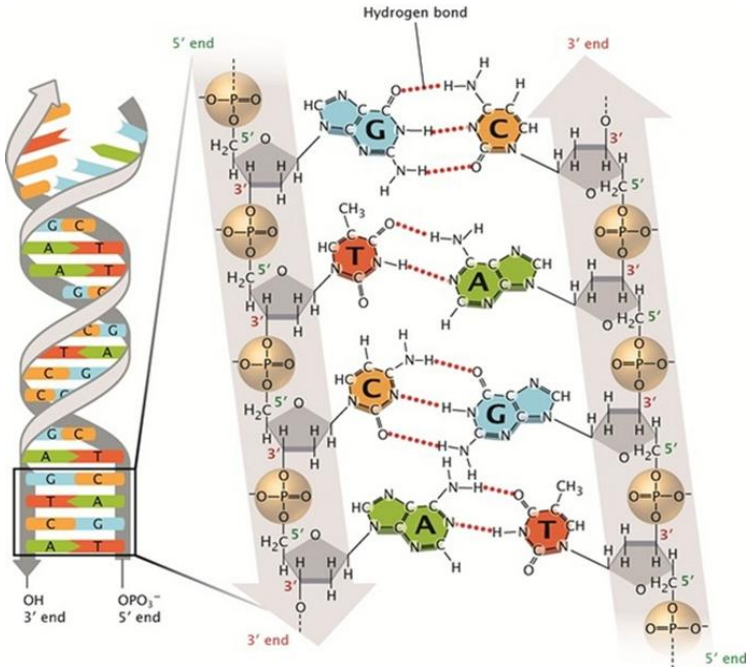

***Figure 1**: Structure of double stranded DNA*

Under physiological conditions (neutral pH, room temperature, up to ~200mM NaCl) DNA adopts B-DNA conformation in aqueous media (Frank-Kamenetskii 1997). The phosphate groups in the DNA backbone (pKa~2) deprotonates in most environmentally relevant solutions (ranging between pH 4-9) and physiological conditions, resulting in a negatively charged backbone (Frank-Kamenetskiĭ et al. 1987; Omoike et al. 2004). The charged DNA polymers (or polyelectrolyte) often exhibit unique molecular properties (Dobrynin und Rubinstein 2005). For instance, due to the repulsion between the negatively charged phosphate groups, DNA behaves like a stiff rod below a certain length known as persistence length (Lu et al. 2001; Singh et al. 2025). With increasing polymer length above the persistence length, DNA polymers increasingly bend and coil. The persistence length of DNA is ~150 bp or 50 nm under physiological conditions (Lu et al. 2001).

The solution chemistry controls the polyelectrolytic properties of DNA polymers. For instance, with increasing ionic strength the negative backbone charge is neutralized resulting in lower persistence length and a higher melting temperature (Messina et al. 2004; Sodnikar et al. 2021). Presence of divalent cations may also promote coiled conformations of DNA by bridging negatively charged backbones (Sodnikar et al. 2021). In living organisms, length of DNA polymers varies over several orders of magnitude. Length of DNA varies from 2 kbp (1kb = 1000 bp) to over 1000 kbp (Mbp) in virus and bacteriophages to 500kbp to 12Mbp in prokaryotes including bacteria to 6 billion bp in humans (Gniazdowska et al. 2013; Sessions 2013).

1.2 Fate of DNA in the environment

Environmental or ancient DNA (aDNA) originates from remnants of living organisms like skin cells, faeces, urine or microfossils (Orlando et al. 2021) and leaves (Poté et al. 2009) root cap cells or pollen (Levy-Booth et al. 2007; Parducci et al. 2013). As cells enter the environment, they may undergo immediate lysis, resulting in the release of their DNA into the surrounding milieu (Nielsen et al. 2007). DNA is a chemically fragile molecule which undergoes constant physical and chemical damages. Inside the living cells, various cellular repair mechanisms continuously operate to repair these damages for proper functioning of biochemical processes (Lindahl 1993). However, once cells die, the cellular repair mechanisms cease to operate, resulting in accumulation of damage in DNA and the loss of genetic information. In the extracellular environment, DNA can follow three primary fates, as described by Pedersen et al. 2015.:

First, it may be degraded through a variety of biotic and abiotic mechanisms.

Second, it can adsorb to environmental surfaces, particularly mineral surfaces, which can promote its long-term persistence (Crecchio und Stotzky 1998; Cai et al. 2006b; Hettiarachchi und Grassian 2024).

Third, incorporation of DNA by microbes where most of the DNA is metabolised as a nutrient source where a small fraction integrates into the host genome resulting in natural transformation or horizontal gene transfer (Lorenz und Wackernagel 1994; Thomas und Nielsen 2005; Pedersen et al. 2015).

Biotic degradation by bacterial DNases is considered as the primary degradation pathway for eDNA (Blum et al. 1997). The enzymatic hydrolysis of the phosphodiester backbone of the DNA leads to the cleavage of the DNA strand between the 3’ hydroxyl group of one nucleotide’s sugar and the 5’ phosphate group of the next nucleotide (Parsiegla et al. 2012). This cleavage of the DNA backbone leads to the fragmentation of extracellular DNA polymers, resulting in DNA fragments ranging from 40 to 500 bp in samples dated between 4 and 13,000 years old (Pääbo 1989; Dabney et al. 2013). Another study shows that aDNA is typically shorter than 100 bp, regardless of sample age (Sawyer et al. 2012). Therefore, with prolonged exposure to degradation, highly fragmented DNA polymers predominate, preferentially at fragment lengths shorter than 100 bp (Deagle et al. 2006; Pietramellara et al. 2009; Dabney et al. 2013; Singh et al. 2025).

In addition to biotic decay, extracellular DNA can also be degraded by various abiotic pathways, such as temperature, UV radiation, and pH (Strickler et al. 2015). While temperature higher than 50 °C may directly degrade DNA, moderate temperature changes also stimulate microbial

metabolism and nuclease activity enhancing enzymatic hydrolysis, which would be an indirect temperature effect (Hofreiter et al. 2001; Strickler et al. 2015). Exposure to ultraviolet-radiation (UV), in particular UV-B light can directly lead to photochemical reactions that damage DNA strands (Häder et al. 2003; Strickler et al. 2015). UV radiation also leads to the formation of reactive oxidant species (ROS) which induce DNA damage (Valko et al. 2006; Sharma et al. 2012). ROS-induced oxidative attack on DNA leads to the oxidation of deoxyribose, strand breakage, removal of nucleotides, modifications of the organic bases of the nucleotides and DNA-protein crosslinks (Sharma et al. 2012). UV radiation also inhibits growth of heterotrophic bacteria or stimulates autotrophic bacteria, which leads to decreasing or increasing production of exonucleases, which indirectly affects enzymatic degradation of eDNA (Sommaruga 2001; Häder et al. 2003; Strickler et al. 2015).

pH is another key abiotic factor influencing DNA stability. Acidic conditions from pH<4 catalyse hydrolytic processes like depurination and phosphodiester bond hydrolysis (Alaeddini et al. 2010; Strickler et al. 2015). In contrast, alkaline conditions may increase eDNA persistence (Mauvisseau et al. 2022). It was also found, that alkaline conditions do not directly cause DNA decay in strict chemical sense but lead to degradation by strand separation (Kasyanenko et al. 2025). Moreover, pH strongly affects exonuclease activity, with enzymes such as DNase I exhibiting optimal activity near neutral pH (Haas et al. 2014), thereby indirectly modulating enzymatic DNA degradation (Mauvisseau et al. 2022; Jo 2026).

Therefore, the fate of DNA in the environment mainly depends on exonuclease activity, modulated by abiotic factors, and the availability of mineral surfaces to stabilize eDNA.

1.3 Environmental relevance of Fe(III)-(oxyhydr)oxides

The adsorption of DNA to mineral surfaces, particularly Fe(III)-(oxyhydr)oxides, has been identified as the key process to stabilize DNA against various degradation pathways, including enzymatic hydrolysis (Cai et al. 2006b; Barrón und Torrent 2013; Hettiarachchi und Grassian 2024). Fe(III)-(oxyhydr)oxides, despite being a minor constituent (by weight) of most soils and sediments, constitutes a major reactive fraction owing to their high specific surface area and high surface reactivity (Liu et al. 2021; Scheinost und Singh 2023). Fe(III)-(oxyhydr)oxides represent a widespread group of nanoscale minerals, including goethite, ferrihydrite and hematite (Barrón und Torrent 2013; Scheinost und Singh 2023). These minerals carry surface hydroxyl groups that can protonate-deprotonate with varying solution pH resulting in variable surface charge that primarily governs their reactivity (Liu et al. 2021). Among these, goethite (α-FeOOH) is the most abundant pedogenic Fe(III)-oxide in soils on a global scale, reflecting its stability under a broad range of environmental conditions (Scheinost und Singh 2023).

The formation of Fe(III)-(oxyhydr)oxides starts with iron being released into the environment by the weathering of Fe^{2+} containing primary or secondary silicate minerals like biotite, pyroxene, amphibole or olivine. Most of the released aqueous iron precipitates as Fe(III)-oxides, after the oxidation to Fe^{3+} and its hydrolysis. Goethite formation is favoured by slow hydrolysis of Fe^{3+} at lower temperatures under aerated, temperate and humic conditions. (Scheinost and Singh 2023). Another pathway of goethite formation is the transformation of the precursor iron oxyhydroxide ferrihydrite by dissolution-reprecipitation or direct recrystallization processes (Barrón and Torrent 2013), driven by humid conditions, high pH and moderate temperatures (Balsam et al. 1995; Schwertmann 2000; Jiang et al. 2016).

Goethite (α-FeOOH) is a Fe(III)-oxide hydroxide and isostructural with diaspore (α-AlOOH) (Cornell und Schwertmann 2006). The crystal structure of goethite is composed of double chains of edge-shared octahedra ($FeO_3(OH)_3$) that are joined to other double chains by sharing corners and hydrogen bonds (Fig. 2A) (Scheinost and Singh 2023). The habit of goethite crystals, as revealed by electron microscopy, can be described as needle-like shape (Fig. 2B) (Hiemstra und van Riemsdijk 1996; Das und Hendry 2011). Numerous studies have used goethite as a model mineral to study DNA-mineral interactions and to address the fate of extracellular DNA in the environment, as goethite exhibits high reactivity for DNA (Omoike et al. 2004; Cai et al. 2007; Schmidt und Martínez 2017; Sodnikar et al. 2021; Feng et al. 2024; Chen et al. 2025).

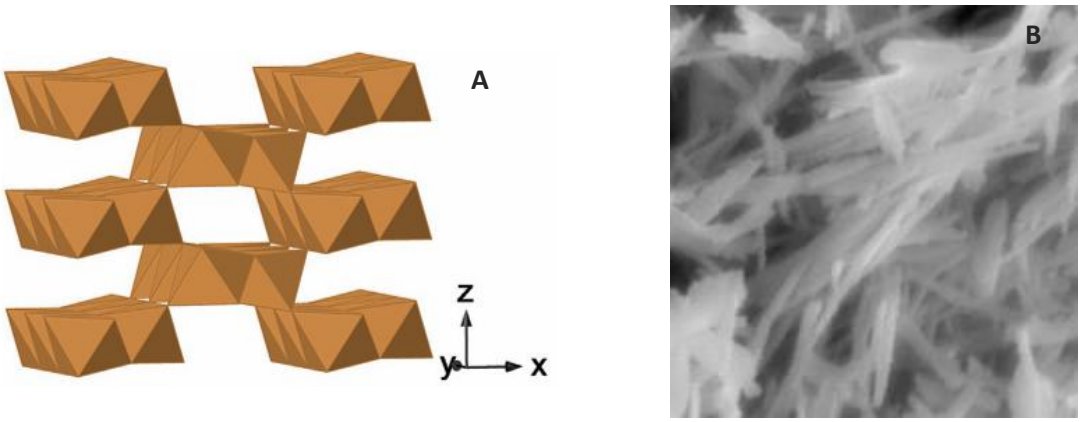

***Figure 2**: A: Crystal Structure of Goethite; B: Needle-shaped habitus of goethite*

1.4 Mechanism of DNA-goethite interaction

Adsorption to soil components, mainly mineral surfaces is considered as a key mechanism that allows the long-term persistence of DNA in the environment. Numerous studies worked on the adsorption of DNA to soils (Cai et al. 2006b; Gardner und Gunsch 2017), clay minerals (Cai et al. 2007; Singh et al. 2025) and Fe(III)-(oxyhydr)oxides (Cai et al. 2007; Schmidt and Martínez 2017; Sodnikar et al. 2021). These studies describe adsorption driven by electrostatic interactions between the sorbent and DNA. For variable-charged mineral surfaces like goethite, the electrostatic interaction between negatively charged DNA and the mineral surface depends on pH. At solution pH below the point of zero charge (PZC), the mineral surface carries a net positive charge and electrostatically attracts negatively charged DNA molecules (Cai et al. 2006a; Saeki et al. 2010). But as pH increases above PZC, surface hydroxyl groups deprotonate, making mineral surface more negative and hence, resulting in lower adsorption of DNA (Sodnikar et al. 2021). Goethite also adsorb DNA via ligand exchange between the phosphate of the DNA backbone and the OH-groups of the goethite surface forming inner-sphere complexes as covalent Fe-O-P bonds (Stumm 1995; Omoike et al. 2004; Schmidt und Martínez 2017; Chen et al. 2025). ATR-FTIR (attenuated total reflectance Fourier transform infrared) spectroscopy shows that these covalent Fe-O-P bonds form preferentially as monodentate complexation, rather than bidentate complexation (Omoike et al. 2004; Schmidt and Martínez 2017), as only one oxygen atom of DNA phosphate group is available for bonding (Omoike et al. 2004). Inner-sphere complex formation plays a major role at higher pH as electrostatic attraction is suppressed with increasing pH (Sodnikar et al. 2021).

The bridging of divalent cations between the negatively charged DNA backbone and negatively charged mineral surfaces is also considered as a relevant adsorption mechanism. On one hand, divalent cations such as Mg^{2+} or Ca^{2+} can form bridges between phosphate groups within the DNA backbone, reducing intramolecular repulsion between negative charges of the polyelectrolyte. This favours electrostatic attraction to negatively charged surfaces and leads additionally to a more compact conformation of the molecule, which reduces its footprint on the mineral surface (see Chapter 1.1), leading to higher adsorption. In addition, divalent cations may enhance DNA adsorption by forming bridges directly between the phosphate groups of the DNA backbone and the negatively charged mineral surface. This adsorption mechanism becomes more pronounced at higher pH values, as mineral surface charge becomes increasingly negative with increasing pH. Even at neutral pH, goethite surfaces can display localized negative charges despite having an overall positive net charge. (Lorenz und Wackernagel 1987; Poly et al. 2000; Franchi et al. 2003; Nguyen und Chen 2007; Saeki et al. 2010; Sodnikar et al. 2021)

Various bonding types like electrostatic attraction and inner-sphere complex formation are rarely exclusive and contribute both to DNA adsorption to goethite (Sodnikar et al. 2021).

1.4.1 DNA-goethite interaction in the presence of competing species

In nature, mineral surfaces are rarely pristine. They are associated with various ions and organic matter (OM) which can change the properties of mineral surfaces and hence affect the interactions of DNA and minerals.

Phosphate is one of the most common inorganic chemical species in natural environments, usually forming insoluble precipitates at high concentrations or strongly adsorbs onto minerals at lower concentrations (Liu et al. 2012; Yagi und Fukushi 2012; Liu et al. 2021). While phosphate concentrations are very low in soil solutions (0.01 – 1 mM) (Ibrahim et al. 2022; Chen et al. 2025), fertilizer leaching (Liu et al. 2012), guano deposits in cave sediments, which serves as a potential source of human aDNA (Gelabert et al. 2025; de-Dios et al. 2025) and bone mineral dissolution (Biswas et al. 2022) can result in elevated phosphate concentrations.

Phosphate is known to be a strong competitor for DNA adsorption onto mineral surfaces especially goethite due to its similar binding mechanism as of DNA (Sodnikar et al. 2021; Chen et al. 2025). Several studies have demonstrated a reduction in DNA adsorption in the presence of phosphate on goethite (Cai et al. 2007; Sodnikar et al. 2021; Feng et al. 2024). Additionally, desorption of previously adsorbed DNA was observed from goethite (Cai et al. 2007; Chen et al. 2025) in the presence of phosphate in solution. Competition between phosphate and DNA for adsorption onto mineral surfaces can occur through two main mechanisms. First, at circumneutral pH, phosphate readily forms inner-sphere complexes with surface hydroxyl groups (Hiemstra und van Riemsdijk 1996; Kim et al. 2011; Chen et al. 2025), which not only reverses the net surface charge of goethite from positive to negative but also reduces the number of hydroxyl groups available to form inner-sphere complexes with DNA, reducing total DNA adsorption (Sodnikar et al. 2021). Second, inorganic phosphate can electrostatically interact with residual positively charged surface sites, and thereby directly compete with phosphate of DNA for binding to surface adsorption sites, promoting desorption (Antelo et al. 2005; Sodnikar et al. 2021).

In addition to inorganic ions, soils and sediments contain substantial amounts of OM, derived from the decomposition of plant and animal residues as well as microbial biomass (Dai et al. 2022). Dissolved organic matter (DOM), an umbrella term for a variety of organic molecules, may form organo-mineral complexes, by adsorbing to the mineral surface, which is consiered as a first step to long-term OM stabilization (Mikutta et al. 2007; Schmidt und Martínez 2018). Kleber et al. 2007 hypothesized a *zonal model* of organo-mineral interactions, where initial

adsorption of OM-molecules to mineral surface may serve as a base for other biomolecules to subsequent adsorption. While Sodnikar et al. 2021 expect OM to compete with nucleic acids at positively charged surfaces, Schmidt and Martínez 2018 highlight biomolecule-biomolecule interactions in solution as a stabilizing mechanism of OM in soils.

Bovine serum albumin (BSA) is a protein that is widely used as a model for soil OM (Schulze 2005; Benndorf et al. 2007; Schmidt und Martínez 2018). Although BSA is not itself a soil protein and does not represent biochemical diversity of soil and sediment proteins, it shares a similar globular structure and molecular mass (~66kDA) with proteins extracted from soils (Schulze 2005; Chourey et al. 2010; Schmidt und Martínez 2018). Furthermore, the isoelectric point of BSA at ~4.7 lies within the range previously reported for proteins extracted from groundwater originating from the effluent of a field reactor (Benndorf et al. 2007; Schmidt and Martínez 2018).

Previous studies have shown that at pH 5 BSA binding to DNA can partially screen intramolecular repulsion between DNA, thereby promoting increased DNA adsorption onto goethite up to a certain BSA concentration. However, beyond this threshold, increasing BSA concentration in solution leads to blocking of binding sites and therefore to competition, which reduces DNA adsorption. In addition, experiments involving the adsorption of DNA-BSA complexes onto goethite suggest that BSA can facilitate adsorption through a bridging mechanism or supramolecular associations, while simultaneously hindering the formation of inner-sphere complexes between DNA and the goethite surface. (Schmidt and Martínez 2018)

Despite this reduced adsorption, or the presence of more weakly bound DNA, OM has been reported to enhance protection against enzymatic hydrolysis compared with inorganic clays (Cai et al. 2006b). This effect is attributed to the incorporation of DNA molecules into three-dimensional macropore structures of organic coated minerals, where DNA becomes less accessible to nucleases (Cai et al. 2006b).

While the interaction of DNA with pristine goethite is widely studied, the interaction of DNA with goethite in the presence of various organic and inorganic species that compete with DNA for surface adsorption sites and its impact on DNA degradation is poorly understood.

1.4.2 Theory of *Trains* and *Loops* as a property of DNA surface adsorption

Unlike the point charges such as phosphate and small biomolecules like BSA, the polyelectrolyte properties of DNA govern its adsorption characteristics. Particularly, stiff DNA polymers below their persistence length, tend to adsorb in a flat conformation, while long and flexible DNA molecules, typically make *loop-train-tail* architecture, where *trains* refer to the section of DNA

lying flat on the surface while *loops* and *tails* hang away from the surface from respective attachment points (Fig. 3). (Jenckel und Rumbach 1951; Hesselink 1977; Sodnikar et al. 2021) According to these findings, it is assumed that longer DNA polymers exhibit a greater proportion of structural elements such as *loops* and *tails* that are not directly attached to the mineral surface, whereas shorter DNA polymers predominantly adsorb in the form of *trains*, with most of their segments in direct contact with the mineral surface. Consequently, substantial parts of long DNA polymers are hanging away from minerals and are therefore assumed to behave similarly to DNA in solution. This distinction has environmental implications in the context of DNA degradation, as DNA segments not bound to the mineral surface are unlikely to be protected from degradation processes through mineral adsorption. This concept is shown in Figure 3, with the model DNA bound to goethite surface via *trains* forming *loops* and *tails* which are more likely to enzymatic degradation, damage by UV radiation or reactive oxidant species (ROS). Phosphate and BSA in the solution may change the behaviour of the solvent-exposed parts of DNA.

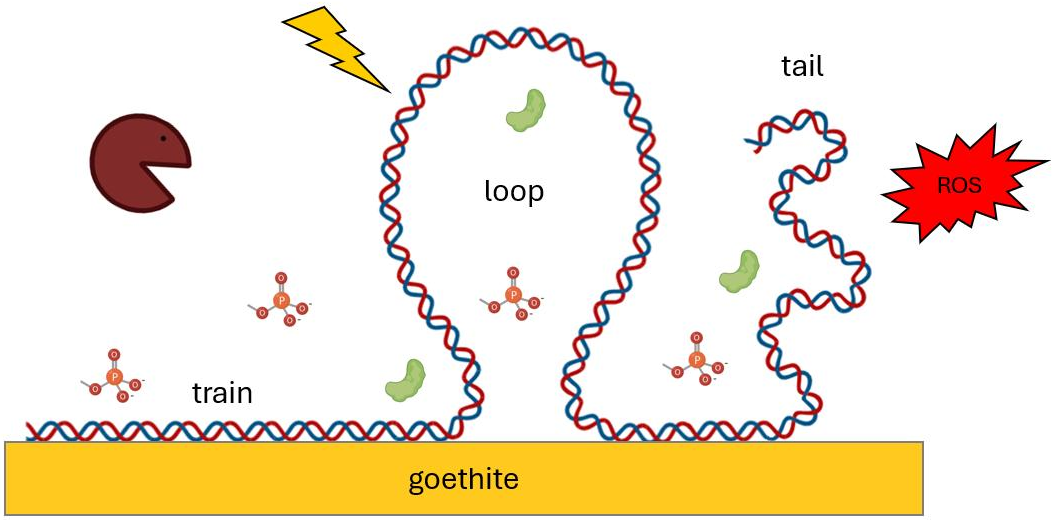

***Figure 3**: Concept of DNA as a polyelectrolyte with trains, loops and tails; parts of the DNA polymer are not attached to the mineral surface (goethite) and therefore unlikely to be protected from degradation processes (enzyme, UV-radiation or ROS (reactive oxidant species))*

2 Research objectives

Adsorption onto mineral surfaces is considered as key mechanism contributing to the long-term persistence of DNA in environmental systems. Over the past decades, numerous studies have investigated the influence of solution chemistry (pH, ionic strength, ion type) (Lorenz and Wackernagel 1987; Nguyen and Chen 2007; Sodnikar et al. 2021; Feng et al. 2024; Chen et al. 2025), mineralogy (Verma et al. 2024; Singh et al. 2025) and molecular properties of DNA including polymer length (Singh et al. 2025) on DNA adsorption. These studies have shown that mineral type, solution chemistry and polymer length of DNA play crucial roles in governing DNA–mineral interactions.

Despite these advances, most of the existing research has focused on DNA adsorption on pristine mineral surfaces under simplified conditions. Natural environments, however, are complex, and mineral surfaces are rarely free of competing inorganic and organic species. While few studies have addressed this complexity by examining DNA adsorption in the presence of competing ions (Sodnikar et al. 2021; Feng et al. 2024; Chen et al. 2025) or OM (Cai et al. 2006a; Cai et al. 2006b; Cai et al. 2007; Schmidt und Martínez 2018) important gaps remain. In particular, the kinetic and thermodynamic aspects of DNA–mineral interactions under competitive conditions and the role of DNA polymer length in this process are still poorly constrained. Additionally, all these works investigated DNA adsorption and concluded that adsorption was crucial for long-term DNA protection but only little studies worked on degradation itself (Demanèche et al. 2001; Dell'Anno und Corinaldesi 2004; Cai et al. 2006b).

Previous studies have investigated the influence of OM and organic rich soils on the adsorption of DNA to mineral surfaces and found that organic rich soils reduce DNA adsorption relative to pristine mineral phases (Cai et al. 2006a; Cai et al. 2006b), primarily due to increased electrostatic repulsion between negatively charged DNA molecules and organic coated clay surfaces (Cai et al. 2006a). Additionally, the formation of supramolecular complexes between DNA and bovine serum albumin (BSA) can inhibit the coordination of DNA phosphodiester groups with goethite surfaces, resulting in decreased DNA adsorption at elevated BSA concentration (Schmidt und Martínez 2018). While some studies on clay suggest that OM may enhance protection of DNA against enzymatic degradation (Cai et al. 2006b), the effect of OM on DNA degradation on goethite is not well studied. Also, consideration of DNA fragment length is necessary at this stage to better understand the extent to which OM–induced stabilization influences DNA persistence on goethite surfaces.

To address these research gaps, DNA fragments of three different lengths were selected. Goethite was used as a model mineral, while phosphate and bovine serum albumin (BSA) were

chosen as model competing species. By combining adsorption experiments conducted in the presence of competing species with complementary degradation studies, this thesis aims to bridge existing knowledge gaps and provide deeper insight into the mechanisms governing DNA–mineral interactions and long-term DNA preservation by addressing following questions:

I. How does DNA polymer length controls adsorption and desorption behaviour on goethite?
II. How does phosphate and BSA impact DNA adsorption kinetics and equilibrium on goethite?
III. How do DNA polymer length and competition jointly shape the susceptibility of goethite-bound DNA to enzymatic degradation?

3 Materials and Methods

3.1 Goethite

Goethite previously synthesized using the chemical precipitation method of Schwertmann and Cornell as described in (Singh et al. 2025) was used for the present study. The specific surface area (SSA) is 37.02 m^2/g.

3.2 DNA

For the present study DNA polymers of three different lengths were used: 99 base pairs (bp), 1000 bp and genomic DNA gDNA (median length approx. 19,000 bp). 99 bp and 1000 bp DNA fragments were synthesised by polymerase chain reaction (PCR), while the sodium salt of gDNA derived from salmon sperm was obtained commercially from Sigma-Aldrich (USA). To prepare gDNA stock solution, gDNA sodium salt was mixed in buffer solution and put in a rotational spinner (30 rpm) for minimum 3 hours to ensure complete dissolution.

To synthesise 99 bp DNA and 1000 bp DNA, pBR322 (Thermo Fisher Scientific, USA) was used as template. All required reagents and their respective volumes for the preparation of the PCR master mix are listed in Table 1. The reaction mixture was prepared by mixing the reagents in a specified order. Ultrapure water (resistivity ≥ 18.2 MΩ.cm) was added first and the DNA polymerase was added last to prevent enzymatic activity prior to thermocycling.

Following this, 50 µL of the PCR master mix was transferred to PCR tube and then loaded in the thermocycler. The PCR was performed according to specific temperature-time profiles, which regulate the denaturation, annealing and extension steps of the reaction. The exact cycling conditions used for synthesising of the 99 bp and 1000 bp fragments are summarized in Table 2. Subsequently, the PCR products were purified using silica spin columns (MinElute PCR Purification Kit (Qiagen, USA) to remove salts, unreacted nucleic acids and polymerase. PCR products were mixed with binding buffer (BB) (57% 5 M guanidine hydrochloride, 40% isopropanol, 3% 3 M Sodium Acetate, pH 5.2) at a ratio of 5:1 (binding buffer to PCR product volume). Aliquots of 750 µL of the PCR-BB solution were transferred into the spin columns and centrifuged for 30 seconds, enabling the DNA to adsorb onto the silica membrane. The spin columns were then washed by centrifugation for 30 seconds with wash buffer (80% ethanol, 20% 10mM Tris-hydrochloride, pH 7.5), effectively removing residual salts from the binding buffer, as well as unincorporated dNTPs, excess primers and enzymes. After washing, only DNA of the desired polymer length remained bound to the silica membrane. Elution was performed by adding HEPES buffer to the columns, incubating for 1 minute and centrifuging for 1 minute into 1.5ml protein Lobind tubes. The elution step was repeated using the eluate to maximize

yield. The resulting DNA solutions were pooled in 2ml protein Lobind tubes and stored at −80°C. All centrifugation steps were carried out at 19,000 rcf. The purified PCR product was analysed for its length, salt contamination and absorbance ratio to ensure the quality.

***Table 1**: reagents and respective volumes for a full batch (96 wells) of DNA synthesis with pBR322 template*

Components	***Volume (µL)***
10x DreamTaq Buffer	480
dNTP Mix, 10 mM each	96
Forward primer, 100 µM	48
Reverse primer, 100 µM	48
Template DNA 2 ng/µL	48
DreamTaq DNA Polymerase	24
Water	4056
Total Volume	**4800**

***Table 2**: thermocycler settings for 99 bp and 1000 bp PCR synthesis*

Step	***No. of cycles***	***°C/min***
Initial denaturation	1	95/1.5
Denaturation	30	95/0.5
Primer annealing		58.5/0.5
Extension		72/1
Final extension	1	72/10

3.3 Analysis

3.3.1 DNA quantification and DNA length

The concentration of DNA was determined by measuring UV absorbance at 260 nm on a Tecan Infinite Pro 200 spectrophotometer (Tecan) with NanoQuant plate using an extinction coefficient of 0.020 $(ng/\mu L)^{-1}cm^{-1}$. Due to higher sensitivity, fluorometric assays (Qubit 1X dsDNA HS, Thermo Fisher) were used to quantify DNA in experimental supernatants of the order of addition experiments and degradation experiments using a polymer-specific calibration curve prepared by serial dilution of stock DNA (120 ng/µL). The assays were performed by mixing 3 µL of sample with 47 µL of 1X dsDNA HS buffer in fluorescent plate and analysed by measuring fluorescence (excitation 480nm, emission 520nm) on a Tecan Infinite Pro 200 spectrophotometer (Tecan). Samples were diluted in ultrapure water as needed to ensure they fell within the linear range of the fluorometric assay and to reduce any potential background interference.

To verify DNA purity following PCR clean-up, absorbance ratios were measured at 260 nm relative to 280 nm and 230 nm. The A260/A280 absorbance ratio ranged between 1.8 and 2.0, indicating no protein contamination, while the A260/A230 ratio between 2.0 and 2.2 confirmed no salt contamination from the binding buffer after PCR clean-up

Length of DNA after PCR synthesis and after enzymatic hydrolysis was determined using automated gel electrophoresis on an Agilent TapeStation 4150 instrument. ScreenTapes were chosen according to the expected range of DNA polymer lengths. To verify the length of synthesised 99 bp and 1000 bp DNA D1000 ScreenTape was used. For analysing degradation products, HSD1000 ScreenTape was used for 99 bp degradation products and HSD5000 and gDNA ScreenTapes were used for 1000 bp and gDNA degradation products.

3.3.2 Phosphate quantification

The stock concentrations of phosphate solution and samples of the phosphate adsorption isotherm were analysed, using the method developed by Murphy und Riley 1962. This single solution method relies on the reaction of inorganic phosphate with an acidic molybdate solution (acidified with ascorbic acid) and the following formation and reduction of phosphomolybdic acid (Murphy and Riley 1962), which can be measure using UV-spectrophotometer. The method was modified for the analysis in Microplate, 96 well, PS, F-Bottom, clear (Greiner), which allows the measurement of multiple samples with a small reaction volume (200 µL). The samples were measured using Tecan Infinite Pro 200 spectrophotometer (Tecan).

3.3.3 BSA quantification

The BSA stock solution was filtered using 0.2 µm sterile filters (Merck Millipore Ltd.). The concentrations of BSA stock solution, BSA adsorption isotherm samples and BSA kinetics samples were measured using Micro BCA™ Protein Assay Kit (thermos scientific) and Tecan Infinite Pro 200 spectrophotometer (Tecan). 150µl of each sample was added to the wells in a 96 well plate. Then, 150µl of the BCA working reagent was added to the wells and mixed with the pipette. Plates were incubated for 2 hours at 37°C and cooled to room temperature subsequently. Absorbance was measured at 562nm.

3.3.4 DNase I quantification

DNase I was analysed using Tecan Infinite Pro 200 spectrophotometer (Tecan) at 260 nm wavelength with NanoQuant plate (Tecan).

3.4 Solution preparation

3.4.1 Buffer solution

All experiments were performed in a background solution with a pH of 7, which was buffered using 3 mM HEPES (4-(2-hydroxyethyl)-1-piperazineethanesulfonic acid) and 30 mM NaCl. After dissolving the HEPES and NaCl, the pH was adjusted to 7 using HCl and NaOH. Following pH adjustment, the buffer solution was filtered using 0.2 µm sterile filters (Merck Millipore Ltd.) and autoclaved for 40 minutes at 121 °C. The buffer solution was stored in the freezer for future use. The buffer solution was then opened only in the sterile bench.

3.4.2 Phosphate solution

The phosphate stock solution was prepared by dissolving sodium dihydrogen phosphate 1-hydrate (NaH_2PO_4) (VWR) in the background of 3mM HEPES and 30mM NaCl. The phosphate stock solution was prepared in 3x at a concentration of 300 mM. After dissolving NaH_2PO_4 in the buffer solution, the pH was adjusted to 7 again using HCl and NaOH. The phosphate stock solution was filtered using 0.2 µm sterile filters (Merck Millipore Ltd.) and stored in the freezer until use.

3.4.3 BSA solution

Stock solution of BSA was prepared by dissolving Bovine Albium (Fr V, pH 5.2 (Millipore) in the background of 3mM HEPES and 30mM NaCl. After mixing BSA with the buffer solution in a 5 ml protein Lobind vial it was dissolved completely at 60 rpm for 30 minutes on a rotational spinner. Solution was later filtered using 0.2µm protein Lobind filter, wrapped in aluminium foil and

stored at 4°C until use. Subsequently the BSA solution was diluted to desired concentrations and measured again. For short storage or during shaking, the vials were wrapped with aluminium foil and kept in the fridge. BSA-solution was prepared fresh for every experiment.

3.4.4 DNase I solution

To prepare enzyme solution for degradation experiments, DNase I (deoxyribonuclease I from bovine Pancreas, Sigma-Aldrich) was weighed in a 2 ml protein Lobind tube and dissolved in the background of 0.5 mM $CaCl_2$ and 2.5 mM $MgCl_2$ and 3 mM HEPES using a rotational spinner at 30 rpm for 30 min. The vial was covered with aluminium foil and kept on ice after dissolving, to avoid enzymatic activity. The DNase I solution was diluted to 500 ng/µl (10x concentration).

3.4.5 Desorption buffer for degradation experiments

Two different desorption buffers at pH 10 were used to desorb DNA following degradation experiments. For 99 bp DNA desorption buffer containing 3 mM tetraborate, 3.3 mM EDTA and 1 mM PO_4 was used, while for 1000 bp and gDNA desorption buffer containing 3 mM tetraborate, 3.3 mM EDTA, and 20 mM PO_4 was used.

3.4.6 Goethite suspension

The goethite suspension was prepared by hydrating the mineral in buffer solution within a glass vial overnight. During mineral-surface hydration, the suspension was gently stirred using a magnetic stirrer at 200 rpm. The suspension was prepared to achieve a final mineral concentration of 2 mg/mL for every experiment. The goethite suspension was ultrasonicated for 3 minutes for a better particle dispersion at 35 kHz (Bandelin Sonorex RK 100, Bandelin electronics, Germany) before use. To maintain homogeneity during pipetting, the glass vial was placed on a magnetic stirrer operating at 900 rpm. To prevent contamination, the addition of mineral to the glass vial and its mixing with the buffer solution were performed under a sterile bench. All glassware/magnets used for preparing solutions or mineral suspensions were acid-washed and autoclaved. Mineral stock solution was freshly prepared for each experiment.

4 Experimental setup

All batch experiments were conducted in duplicates and run parallelly on a horizontal shaker at 21 °C and 150 rpm. All batch experiments were set-up inside a laminar flow hood to ensure sterile conditions, particularly given the long experimental durations and repeated sampling required for the order of addition experiments. Experiments were performed in 2 mL protein Lobind tubes, which were placed in racks and wrapped with aluminium foil to prevent exposure to light causing potential photochemical reactions. For each experiment no-mineral controls were included to ensure DNA stability over experimental timeframe. All experiments were conducted with the buffer solution and the mineral suspension described above**.** At the end of the experiments, all mineral-DNA/BSA/phosphate samples were centrifuged at 20,000 rcf for 20 minutes. The supernatants were collected and either immediately analysed or stored at −80 °C. DNA samples stored at −80 °C and not immediately analysed were defrosted for at least 1 hour to equilibrate with room temperature, then centrifuged for 1 minute at 20,000 rcf and gently vortexed prior to DNA analysis.

4.1 Adsorption of DNA, phosphate and BSA on goethite

4.1.1 DNA adsorption isotherm

To study the effect of varying DNA polymer lengths on adsorption to goethite, DNA adsorption isotherms were performed with 99 bp DNA, 1000 bp DNA and gDNA. Goethite suspension and DNA solution were mixed in equal volumes to a final batch volume of 100 µL, for 18h. Initial DNA concentrations ranged from 10 to 150 ng/µl. The adsorbed DNA on goethite was calculated as the difference between the initial DNA concentration and the DNA concentration remaining in the supernatant.

4.1.2 Phosphate adsorption isotherm

The phosphate adsorption isotherm was conducted to determine the affinity of phosphate for goethite under the given experimental conditions and to choose relevant phosphate concentrations for further experiments. Goethite suspension and phosphate solution were mixed in equal volumes to a final batch volume of 400 µl, for 18h. The initial phosphate concentrations in the batch reactors ranged between 0.04 – 5mM at pH 7. The samples were analysed and stored at -80 °C. The adsorbed phosphate on goethite was calculated as the difference between the initial phosphate concentration and the phosphate concentration remaining in the supernatant.

4.1.3 BSA adsorption isotherm and kinetics.

For BSA, adsorption isotherm and adsorption kinetics were conducted. For the adsorption isotherm, goethite suspension and BSA solution were mixed at equal volumes to achieve a final batch volume of 200 µL, for 18h. The initial BSA concentrations in the batch reactors ranged between 25 – 350 ng/µl at pH 7. The adsorbed BSA on goethite was calculated as the difference between the initial BSA concentration and the BSA concentration remaining in the supernatant. For the adsorption kinetics, goethite suspension and BSA solution were mixed at equal volumes to a total batch volume of 3000 µL with a final BSA concentration of 300 ng/µL in 5 mL protein Lobind tubes. The goethite-BSA suspension was thoroughly mixed. Samples were collected at 1, 10, 30, and 60 minutes, and at 2, 6, 24, and 48 hours. At each time point, the suspension was gently inverted and mixed before sampling.

4.2 Order of Addition Experiments

Order of addition experiments (hereafter referred to as DNA first and DNA second experiment) were performed to investigate the influence of sequence of addition of DNA and phosphate on adsorption of DNA on goethite. The influence of competing species on DNA adsorption to goethite can be investigated by conducting equilibrium adsorption studies in the three-component system, comprised of DNA, the competing species and goethite. To determine the equilibrium state of DNA adsorption in the presence of competing species, both adsorption (DNA second) and desorption kinetics (DNA first) were conducted in parallel. By changing the order of addition, it is possible to approach equilibrium from both directions and investigate the influence of sequence of addition. This approach helps to confine the actual equilibrium state even when true equilibrium cannot be reached or cannot be attained within a practical timeframe.

For the order of addition experiments equal volumes of DNA (final concentration 40 ng/µl), phosphate (final concentration of 0.1 and 1 mM) or BSA (final concentration of 2 and 200 ng/µl) and goethite (final concentration 2 mg/ml) were combined. For the DNA first experiment, DNA was added to the goethite suspension and allowed to equilibrate for 18 hours before phosphate/BSA was introduced. In contrast, for the DNA second experiment, phosphate/BSA was added first and equilibrated similarly before the addition of DNA. Following the addition of the second component in both cases, 20 µL aliquots were taken at regular intervals, from 1 hour up to 3 weeks (504 hours), for analysis.

4.3 DNA adsorption with respect to the concentration of competing species

4.3.1 DNA adsorption as a function of phosphate concentration

In addition to order of addition experiments, the effect of a broad range of phosphate concentration on DNA adsorption on goethite was investigated.

Experiments were conducted with three DNA polymer lengths (99 bp, 1000 bp, gDNA) across a range of phosphate concentrations, 0.01 to 100 mM. For this DNA was preadsorbed on goethite for 18 hrs. Subsequently phosphate solution of the desired concentrations was added to reach a total batch volume of 90 µl (40 ng/µl DNA, 2 mg/ml goethite). After adding phosphate solution, the batches were incubated again on the horizontal shaker for 100h before sampling. The phosphate concentrations and the incubation time of 100h were chosen based on the results of the order of addition experiments which showed that for all DNA polymers the system reached near-equilibrium conditions within this time frame.

4.3.2 DNA adsorption as a function of BSA concentration

To investigate the competition of DNA polymers and BSA for adsorption on goethite with respect to the DNA polymer length, DNA adsorption as a function of BSA concentration experiments were performed. Experiments were conducted with three DNA polymer lengths (99 bp, 1000 bp, gDNA) across a range of BSA concentrations ranging from 0 to 200 ng/µl. First equal volumes of BSA solution of the desired concentration and mineral suspension were mixed and incubated on the horizontal shaker for 18h. Subsequently DNA solution was added to reach a total batch volume of 90 µl (40 ng/µl DNA, 2 mg/ml goethite). After adding DNA solution, the batches were incubated again on the horizontal shaker for 100h before sampling. The BSA concentrations and the second incubation time of 100h were chosen based on the results of the order of addition experiments. The samples ware measured using Qubit 4 Fluorometer (Thermo Fisher) and Broad Range buffer (Thermo Fisher), according to the protocol provided by the manufacturer.

4.4 Enzymatic degradation experiments

Enzymatic degradation experiments were performed to investigate the effect of BSA and phosphate on degradation of DNA on goethite. Experiments were conducted with three DNA polymer lengths (99 bp, 1000 bp, gDNA) and across a range of phosphate (0, 0.01, 0.1 and 1 mM) and BSA concentrations (0, 20, 50, 100 and 200 ng/µl). For degradation studies, equal volumes of phosphate or BSA solution were mixed with goethite and equilibrated for 18h. After the phosphate/BSA equilibration step, DNA solution was added to the vial, to reach a total batch volume of 90 µl (40 ng/µl DNA, 2 mg/ml goethite).

After 100h, DNase I solution was added to DNA-phosphate/BSA-goethite suspension to reach final DNase I concentration of 50 ng/µl and a total batch volume of 100 µl .The suspension was mixed using a pipette and incubated on the horizontal shaker at 37 °C for 1 hour to ensure optimal enzyme activity. Subsequently, a desorption buffer was added, and the suspension was heated to 75 °C for 10 minutes to deactivate the enzyme due to the combined effects of EDTA and elevated temperature. Finally, the system was incubated at 50 °C for 1 hour to promote DNA desorption.

5 Results

5.1 Adsorption isotherms

5.1.1 DNA

Adsorption isotherms of DNA on goethite (Fig. 4A) were performed to investigate the binding affinity and capacity of DNA to goethite and the effect of polymer length on DNA adsorption. It was observed that DNA adsorption on goethite is polymer length dependent, similar to what was observed in previous studies (Singh et al. 2025). 99 bp DNA adsorbed the least with adsorption maximum at 81.82 ± 0.41 ng/cm^2 while longer DNA polymers adsorbed significantly more at an adsorption maximum of 105.09 ± 0.06 ng/ cm^2 for 1000 bp DNA and 115.42 ± 2.28 ng/ cm^2 for gDNA. Based on the adsorption isotherm, the DNA concentration of 40 ng/µl was chosen for further experiments. At this concentration, surface coverage is close to saturation for 99 bp DNA and ensures complete adsorption for longer DNA polymers.

5.1.2 Phosphate

The adsorption isotherm of phosphate was performed to determine the affinity and capacity of phosphate to goethite in our experimental system. The initial concentrations for the phosphate adsorption isotherm (Fig. 4C) ranged between 0.04-5 mM phosphate. There was complete adsorption below 0.16 mM phosphate. Based on the isotherm data, initial phosphate concentrations of 0.1 mM and 1 mM were selected for further experiments. They represent low and medium surface coverage of phosphate on goethite.

5.1.3 BSA

To determine the affinity and capacity of BSA on goethite, both adsorption isotherm (Fig. 4B) and adsorption kinetics (Fig. 10, SI) of BSA on goethite were performed. The initial concentrations for the BSA adsorption isotherm ranged between 25 and 350 ng/µl and showed maximum adsorption of 214.58 ± 5.83 ng/cm^2. There was complete adsorption until 150 ng/µl BSA. The adsorption kinetics data show that BSA adsorption onto goethite happens very rapidly, reaching the plateau within one minute. Based on isotherm BSA concentrations of 2 and 200 ng/µl were chosen, corresponding to low and complete surface saturation on goethite.

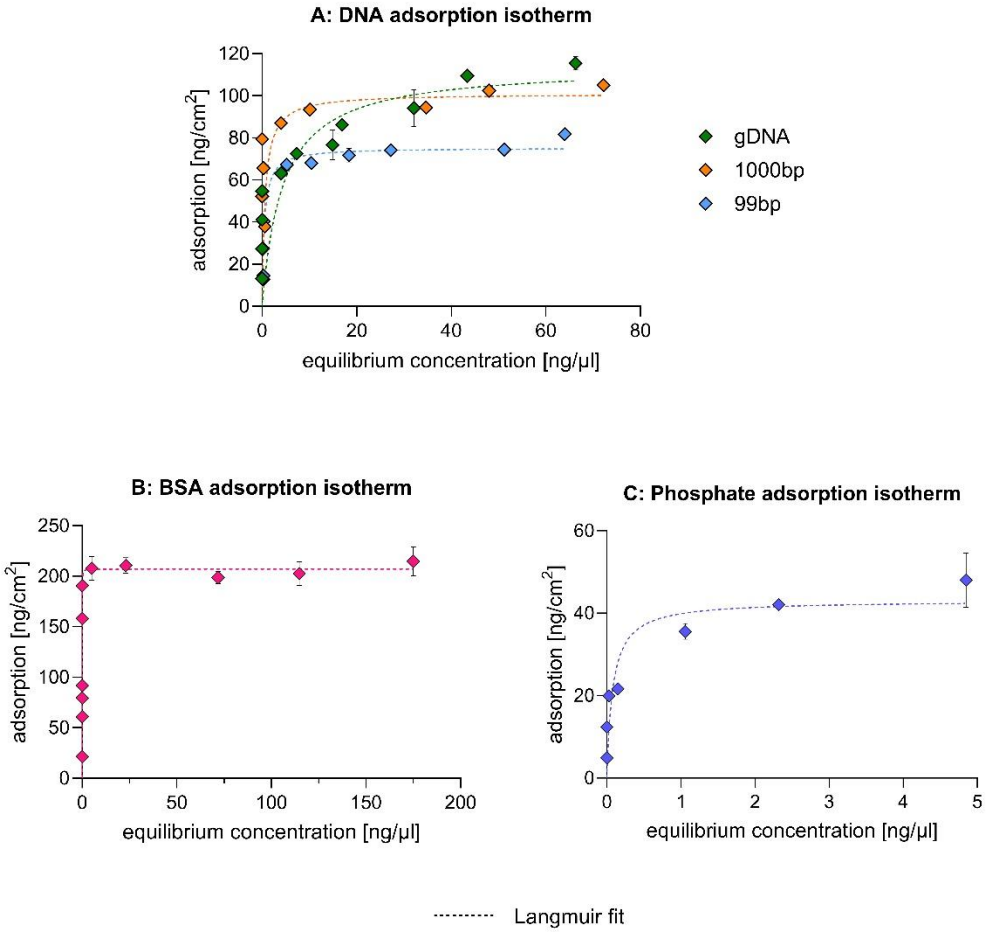

***Figure 4**: A. Adsorption isotherm of 99 bp DNA, 1000 bp DNA and gDNA on goethite with initial DNA concentrations ranging between 10 and 150 ng/µl at pH 7 for 18h incubation. B: Adsorption isotherm of BSA on goethite with initial BSA concentrations ranging from 25 to 350 ng/µl at pH 7. C: Adsorption isotherm of phosphate on goethite with initial phosphate concentrations ranging from 0.04 to 5 mM at pH 7 for 18h incubation. All experiments were conducted in a background solution containing 30 mM NaCl and 3 mM HEPES*

5.2 Order of Addition Experiments

Order of addition experiments were performed to investigate the influence of sequence of addition of DNA and phosphate (0.1 and 1 mM) or BSA (2 and 200 ng/µl) on adsorption of DNA on goethite and to define the equilibrium conditions of the system. Three DNA polymer lengths (99 bp, 1000 bp, gDNA) were selected to investigate its effect on DNA adsorption to goethite. Changing the sequence of addition was intended to define the limits of equilibrium, between adsorption and desorption kinetics if both trajectories do not converge within the given timeframe.

5.2.1 In the presence of phosphate

Figure 5 summarises the influence of phosphate on DNA adsorption kinetics on goethite. From the DNA adsorption isotherm, it was observed that on bare goethite, irrespective of length, there was 100% adsorption at the selected DNA concentration (40 ng/µL). In contrast, the presence of phosphate, irrespective of the order of addition, reduced the extent of DNA adsorption on goethite for all DNA polymers.

At low phosphate concentration (0.1 mM), when phosphate was added prior to 99 bp DNA, only ~20% of added DNA adsorbed. In contrast, when phosphate was added after the adsorption of 99 bp DNA, the extent of adsorption decreased from 100% in the absence of phosphate to ~30%. Additionally, adsorption trend plateaued rapidly when DNA was added after phosphate, within 1 hour, compared to when DNA was added first, which took ~168 hours. Figure 5B shows a similar pattern for adsorption for 1000 bp DNA, when DNA was added second following the preadsorption of 0.1 mM phosphate, where ~20% of DNA was adsorbed during the experimental time frame. However, desorption (1000 bp DNA first) was much less pronounced with ~60% remaining adsorbed after 504h. Contrary to 99 bp DNA and 1000 bp DNA, gDNA in Figure 5C showed no measurable desorption at low phosphate concentration when gDNA was adsorbed first and adsorption extent, when gDNA was added second, was substantially more compared to shorter DNA polymers, with approximately 80% gDNA remaining adsorbed.

Figure 5D-F show the effect of higher phosphate concentration (1 mM) on adsorption of DNA to goethite. In Figure 5D (99 bp DNA) the points are converging at 0% DNA adsorption due to high phosphate concentration and complete desorption (DNA first). In the same way as in Figure 5A with 0.1 mM phosphate, desorption proceeds slower than adsorption, with both processes converging after 100h. Adsorption of 1000 bp DNA on goethite following preadsorption of 1 mM phosphate (DNA second) in Figure 5E shows a similar pattern compared to 99 bp again, showing no adsorption during the experimental timeframe. Adding 1000 bp DNA first, followed by 1 mM

phosphate shows higher desorption (DNA first) of 1000 bp DNA compared to Figure 5B, with ~9.0% DNA remaining bound to the goethite surface. In Figure 5E with 1 mM phosphate 1000 bp DNA desorption (DNA first) reaches the plateau after 100h, showing a faster and more extensive desorption process with higher phosphate concentration. Following the trend with 1 mM phosphate, gDNA shows less adsorption to goethite with preadsorbed phosphate (DNA second) in Figure 5F with ~20% DNA being adsorbed compared to the experiment with 0.1 mM phosphate as described in Figure 5C. Again, desorption (DNA first) proceeds slower than adsorption for gDNA, reaching the plateau after 168h with ~35% remaining adsorbed.

As shown in Figure 5A-F converging curves could be observed only at 1 mM phosphate and with 99 bp and 1000 bp DNA. For 0.1 mM phosphate the possible equilibrium can be constrained within 30.28 ± 2.06% - 19.03 ± 4.38%, 62.46 ± 5.06% - 19.72 ± 5.76% and 99.30 ± 0.1% - 79.47 ± 4.17% DNA adsorption for 99 bp, 1000 bp and gDNA, respectively. For 1 mM phosphate and gDNA the limits are at 35.44 ± 2.28% and 16.23 ± 3.19% DNA adsorption.

Based on the order of addition experiments with phosphate, an equilibration time of 100h was selected for future experiments, acknowledging that in most cases the system remains kinetically controlled. It was accepted that subsequent experiments would therefore not necessarily begin under equilibrium conditions.

5.2.2 In the presence of BSA

Figure 6 summarizes the influence of 2 and 200 ng/µl BSA on DNA adsorption kinetics on goethite. It was observed that irrespective of its concentration, BSA could not displace preadsorbed DNA from goethite, within the experimental time frame. When DNA is added first, followed by BSA, DNA remains bound to the goethite surface. When DNA is added second, following preadsorption of 2 ng/µl BSA, Figure 6A-C show 100% DNA adsorption for all three DNA polymer lengths.

At a high BSA concentration (200 ng/µl), the adsorption of 1000 bp DNA and gDNA is not affected by preadsorbed BSA. In contrary, 99 bp DNA adsorption is reduced to 66.28 ± 1.35%.

At 2 ng/µl BSA concentration, irrespective of DNA polymer length, the system reached equilibrium at 100% DNA adsorbed on goethite with preadsorbed BSA (DNA second). While equilibrium was reached rapidly for 99 bp and 1000 bp DNA, gDNA reached equilibrium conditions after 24h. At 200 ng/µl BSA, 1000 bp DNA and gDNA reached equilibrium with 100% DNA adsorbed onto goethite, after 48h. While 99 bp DNA was far from equilibrium conditions within the experimental time frame, equilibrium can be constrained between 100 ± 0.02% and 66.28 ± 1.35%.

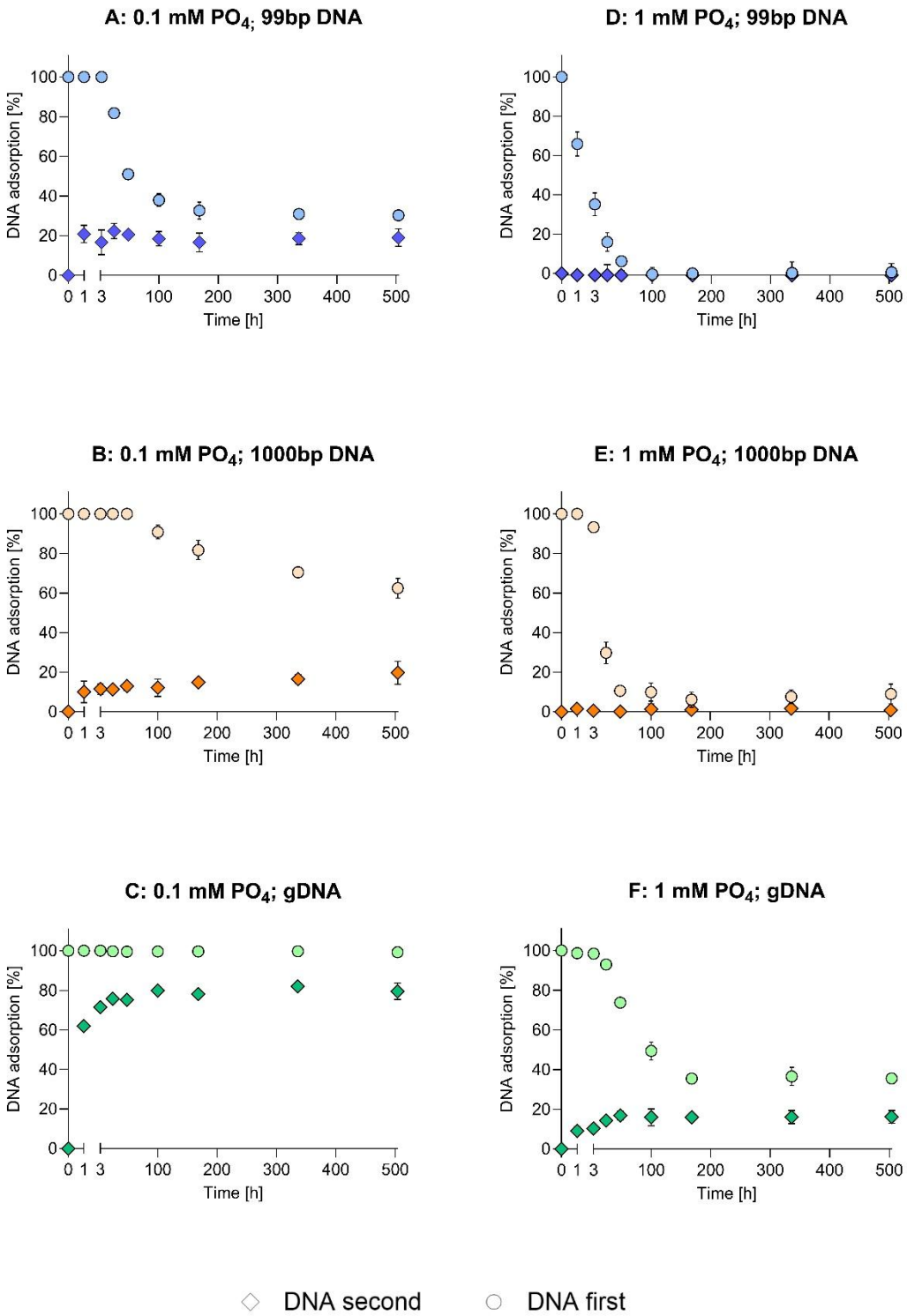

***Figure 5**: Kinetics of DNA adsorption on goethite as affected by the order of addition of DNA and phosphate. (A-C) 99 bp DNA, 1000 bp DNA and gDNA asorption on goethite in the presence of 0.1 mM phosphate. (D-E) 99 bp DNA, 1000 bp DNA and gDNA adsorption on goethite in the presence of 1 mM phosphate. All experiments were conducted in a background solution containing 30 mM NaCl and 3 mM HEPES. Data points and error bars represent mean and range of duplicates run in parallel*

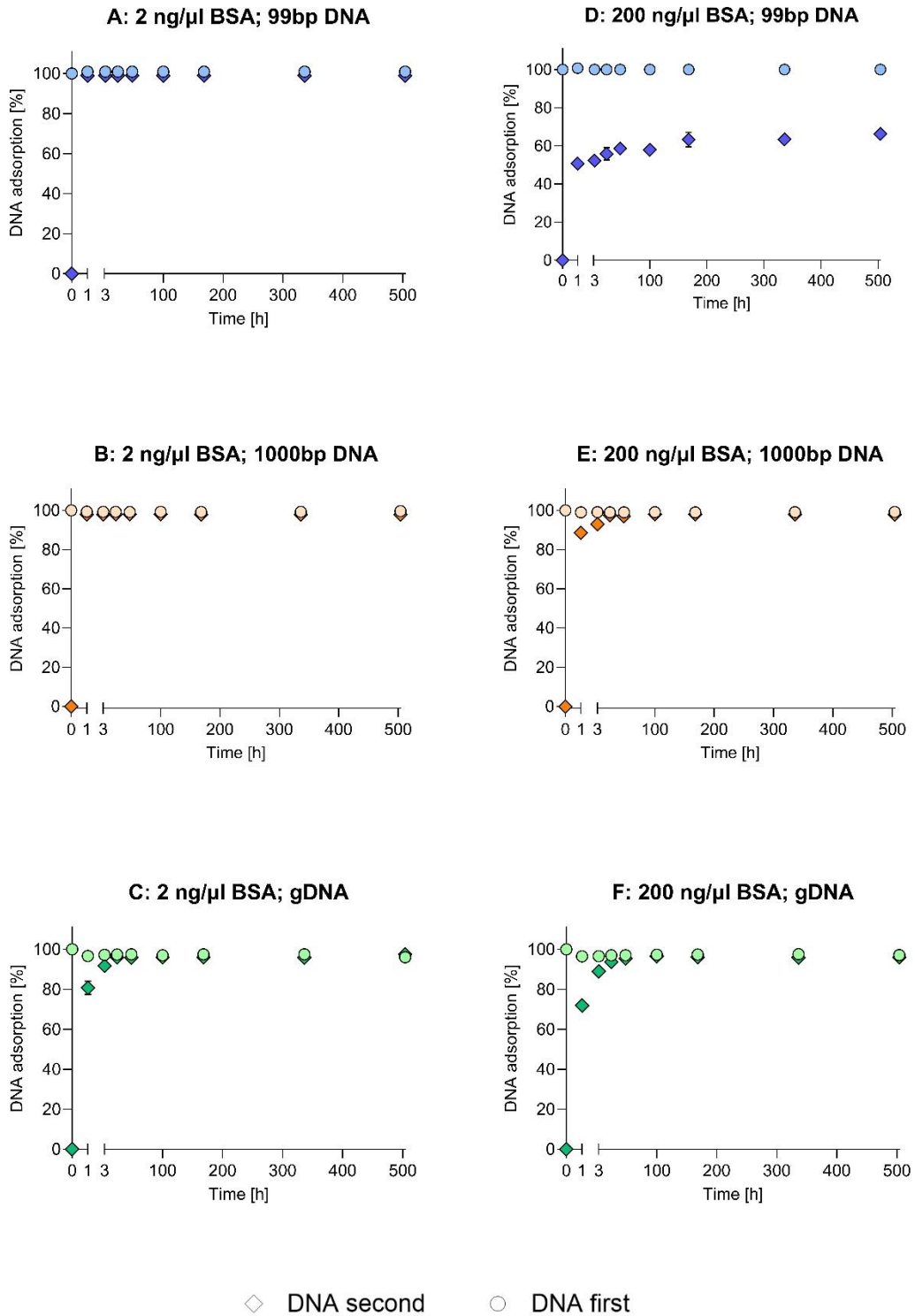

***Figure 6**: Kinetics of DNA adsorption on goethite as affected by the order of addition of DNA and phosphate. (A-C) 99 bp DNA, 1000 bp DNA and gDNA sorption on goethite in the presence of 2ng/µl BSA (D-E) 99 bp DNA, 1000 bp DNA and gDNA adsorption on goethite in the presence of 200 ng/µl BSA. All experiments were conducted in a background solution containing 30 mM NaCl and 3 mM HEPES. Data points and error bars represent mean and range of duplicates run in parallel*

5.3 DNA adsorption as a function of phosphate concentration (DNA first)

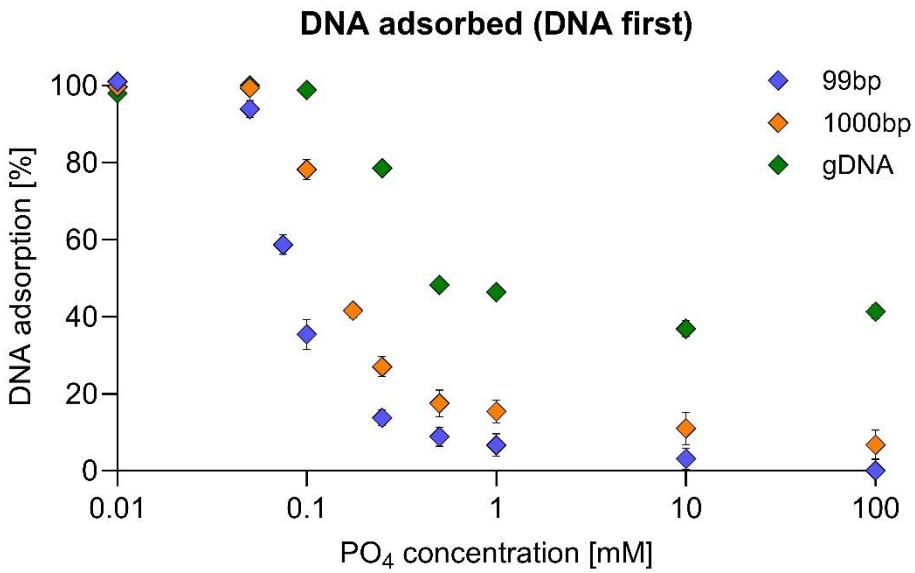

***Figure 7**: Adsorption of 40 ng/µl of 99 bp DNA, 1000 bp DNA and gDNA on goethite at phosphate concentrations ranging from 0-100 mM; DNA was preadsorbed for 18h followed by the adsorption of phosphate for 100 h.*

Since previous experiments showed that phosphate strongly competes with DNA, the current experiment aimed to investigate the competition of phosphate with DNA, by extending the concentration range from 0.01 to 100 mM phosphate. It is important to note that the desorption experiment was performed for 100h, within which the equilibrium may not be attained (Fig. 5). The data of the *DNA adsorption as a function of phosphate concentration* experiment are therefore used to compare phosphate-induced desorption of different polymer lengths at the timepoint 100h. The experimental data of Figure 7 show a substantial reduction in extent of DNA adsorption with increasing phosphate concentration for all DNA polymer lengths. Using 100 mM phosphate leads to a maximum DNA desorption of 100 ± 3.03%, 93.24 ± 3.83% and 58.66 ± 1.85% for 99 bp, 1000 bp and gDNA respectively. Shorter DNA polymers are desorbed better following the trend 99 bp>1000 bp>gDNA. The longer DNA polymers 1000 bp and gDNA do not desorb completely at 100 mM phosphate at pH 7. They show a non-desorbable fraction of DNA under experimental conditions, while 99 bp DNA desorbs completely.

5.4 Enzymatic hydrolysis of DNA in the presence of competing species

Enzymatic hydrolysis experiments were performed to evaluate the effect of phosphate and BSA on the degradation of DNA. For these experiments phosphate and BSA of different concentrations were preadsorbed on goethite and later 40 ng/µl DNA (99 b0, 1000 bp, gDNA) was adsorbed. To analyse DNA degradation, a fluorometric assay that quantifies total DNA irrespective of fragment length and automated gel electrophoresis were used to determine the fragment length distribution after degradation.

5.4.1 DNA degradation in the presence of phosphate

Figure 8 shows, % DNA adsorbed with respect to total DNA that was added initially and % degraded DNA with respect to initially adsorbed DNA in the presence of phosphate. DNA adsorption decreases with increasing phosphate, as already seen in the order of addition experiments. There are two trends to observe. First, DNA degradation increases with increasing phosphate concentration. At 0.1 mM and 1 mM phosphate there was 100% DNA degradation, irrespective of the DNA length. Second, DNA degradation depends on polymer length. In the absence of phosphate and at very low phosphate concentrations there is increasing DNA degradation with increasing polymer length: 99 bp<1000 bp<gDNA

Electropherograms in Figure 8D-F show the size distribution of DNA after enzymatic hydrolysis. In line with the quantitative fluorescence data, due to complete degradation, no DNA was observed on electropherograms at 0.1 and 1 mM phosphate for all three DNA lengths. It can be observed for 99 bp and 1000 bp DNA at 0 and 0.01 mM phosphate, that the intensity of the peaks at its original size (bp) decrease after degradation. In addition to the decrease in the peak intensity after degradation, electropherogram also shows the degradation products. Figure 8D shows a broad size distribution of degradation products for 99 bp DNA with 0 and 0.01 mM phosphate between 25 and 100 bp, while no peak can be observed in the presence of 0.1 and 1 mM phosphate. The degradation products of 1000 bp DNA and gDNA peak at ~100 bp. Both peaks show a right skewed size distribution with pronounced tails towards larger DNA fragments. This is more pronounced for the degradation products of gDNA.

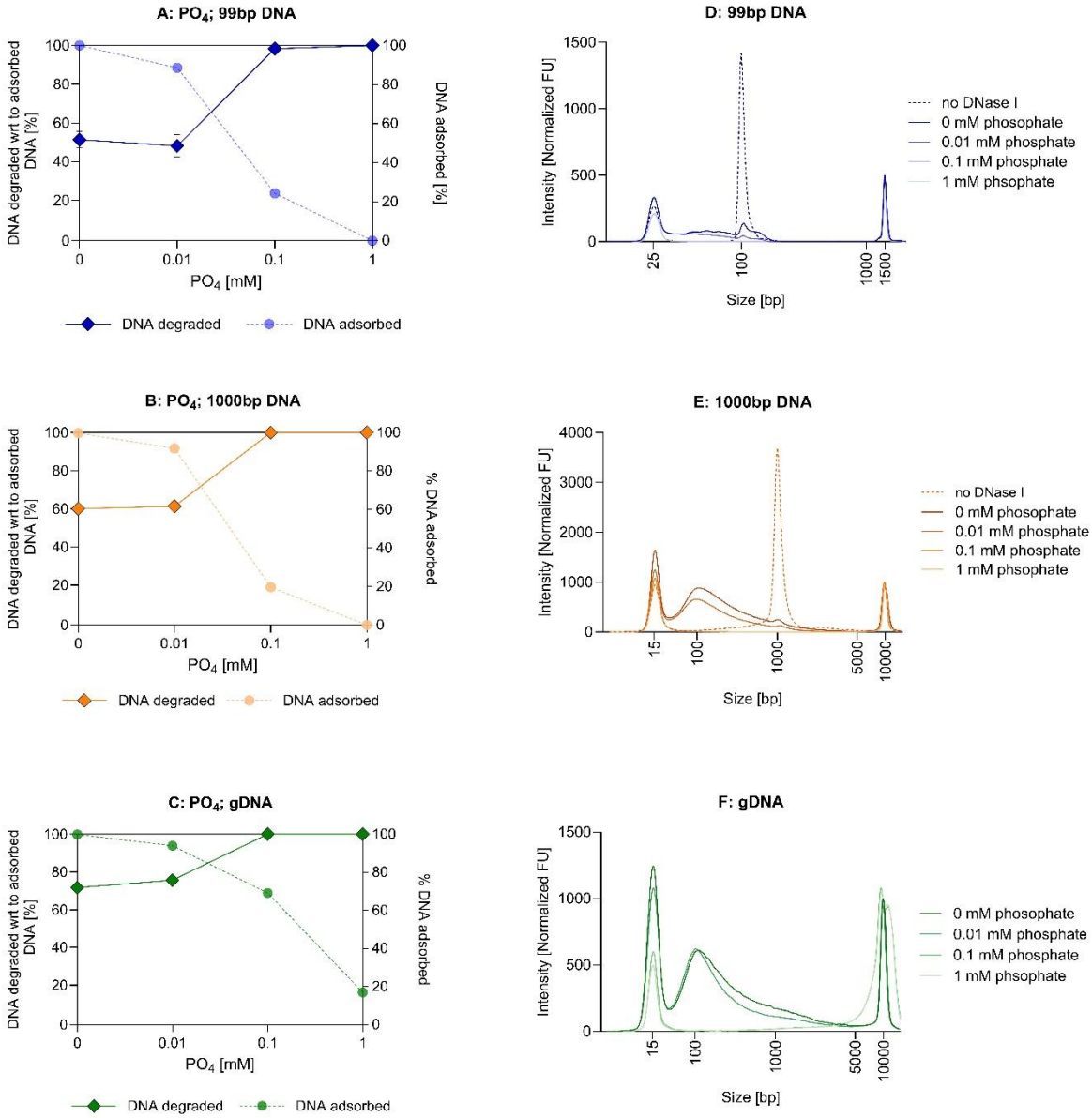

***Figure 8**: Enzymatic hydrolysis of 40 ng/µl DNA on goethite at different phosphate concentrations ranging from 0-1 mM at DNase I concentration 50 ng/µl: (A-B) % DNA adsorbed and % DNA degraded (D-F) Electropherogram of DNA after enzymatic hydrolysis for 99 bp DNA, 1000 bp DNA and gDNA*

5.4.2 DNA degradation in the presence of BSA

Analogue to the degradation experiment with phosphate, DNA degradation experiments with preadsorbed BSA were performed (Fig. 9). For gDNA and 1000 bp DNA it is observed that there is almost 100% DNA adsorption up to BSA concentration of 100 ng/µL, but some DNA was left unadsorbed at highest BSA concentration. Enzymatic hydrolysis increases with increasing BSA concentration. For 1000 bp DNA degradation increases from ~60% in the absence of BSA to ~80% at highest BSA concentration. Degradation of gDNA increases from ~75% to 85% respectively. The percentage of DNA degradation increases between 0 and 100 ng/µl BSA while adsorption remains nearly constant at approximately 100%. For 99 bp DNA, DNA adsorption decreased from 100% at 0 and 20 ng/µl BSA continuously to ~65% at 200 ng/µl BSA. However, contrary to 1000 bp DNA and gDNA, the %DNA degraded remained similar irrespective of the presence or absence of BSA.

The graphs in figure 9D-F illustrate the fragment size distribution obtained after enzymatic hydrolysis in the presence of BSA. For the 99 bp DNA, degradation results in a pronounced reduction in peak intensity relative to the control without DNase I. This peak decreases slightly with increasing BSA concentration but remains largely stable between 20 and 200 ng/µl BSA. Additionally, Figure 9D indicates that the resulting degradation products span a broad size range from 25 to 100 bp.

For the 1000 bp DNA, a substantial reduction of the original 1000 bp peak is observed upon enzyme addition compared with the control. In contrast to the 99 bp DNA, the peak corresponding to the original fragment size disappears completely in the presence of BSA. The degradation products are primarily centered around ~100 bp, with a noticeable peak shift between the sample lacking BSA and those containing increasing BSA concentrations. Specifically, the peak shifts towards shorter fragments from 0 to 20 and 50 ng/µl BSA, while remaining relatively stable at 100 and 200 ng/µl.

A comparable trend is observed for gDNA. As shown in Figure 9F, gDNA degradation products ranged in size 100bp to around 5000bp, with a peak around 100bp. Increasing BSA concentration leads to a slight shift of the fragment distribution towards smaller polymer sizes. The degradation products presented in Figures 9E and 9F display right-skewed size distributions, characterized by tails extending towards longer fragments. With increasing BSA concentration, however, the gDNA degradation pattern becomes more uniform, converging toward a distribution with a dominant peak around 100 bp.

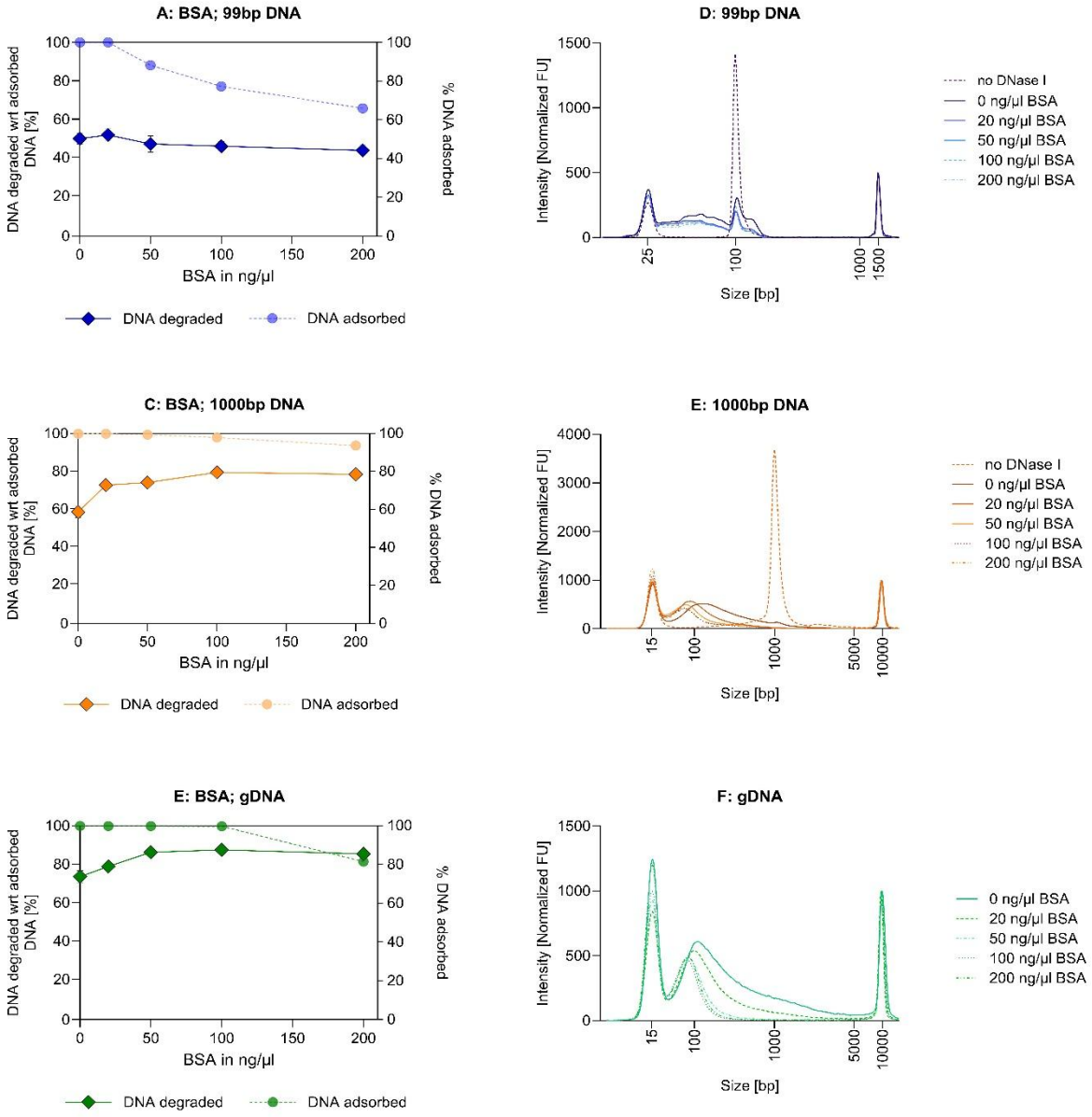

***Figure 9**: Enzymatic hydrolysis of DNA on goethite at different BSA concentrations ranging from 0-200 ng/µl at DNase I concentration 50 ng/µl: (A-B) % DNA adsorbed and % DNA degraded (D-F) Electropherogram of DNA after enzymatic hydrolysis for 99 bp DNA, 1000 bp DNA and gDNA. DNA was adsorbed at the initial concentration of 40 ng/µl.*

6 Discussion

The aim of this thesis is to investigate how polymer length and competing species shape the interactions between DNA and goethite and how both influence the enzymatic degradation of DNA on goethite.

Adsorption to mineral surfaces has been identified as an important process protecting DNA against degradation in the environment (Cai et al. 2006b; Cai et al. 2007; Hettiarachchi and Grassian 2024). Fe(III)-(oxyhydr)oxides, particularly goethite, considering its ubiquity in the environment, reactive surface area and strong affinity for DNA play a critical role in determining persistence of DNA in the environment. Therefore, investigating the dynamics of DNA adsorption on goethite is essential to understand the fate of DNA in the environment. DNA is expected to become increasingly fragmented with prolonged environmental exposure (Pääbo 1989; Dabney et al. 2013; Deagle et al. 2006) and as DNA polymer length is known to strongly affect adsorption to mineral surfaces (Singh et al. 2025), it is necessary to include the effect of DNA polymer length. Furthermore, natural systems do not contain pristine goethite instead, they include a variety of competing ions and OM, which can further modulate DNA and mineral interaction, which indicates that the fate of DNA in the environment depends not only on various degradation pathways and the crucial role of DNA-mineral associations, but also on the dynamics of competing ions and OM.

Following this background, this thesis addresses three central aspects: (I) how DNA polymer length controls adsorption and desorption behaviour of DNA on goethite, (II) how inorganic and organic species, represented by phosphate and BSA, compete with DNA and shape adsorption equilibria and (III) how both aspects shape the susceptibility of goethite-bound DNA to enzymatic degradation.

The discussion section proceeds in two parts. First, adsorption of DNA to goethite will be discussed, examining the effect of DNA polymer length and competing species. In the second section, enzymatic degradation of DNA on goethite will be evaluated, discussing again the effects of polymer length as well as competing species. In contrast to similar studies, that worked on DNA adsorption/desorption with or without phosphate (Schmidt and Martínez 2017; Sodnikar et al. 2021) or BSA (Schmidt and Martínez 2018) this thesis expanded the timeframe to 504 hours compared to minutes.

6.1 Effect of polymer length and competing species on DNA adsorption on goethite

Overall, from the isotherms and order of addition experiments it is evident, that longer DNA polymers adsorb more than shorter ones on pure goethite or in the presence of competing species. This increased adsorption can be explained by the concepts of “chain stiffness” and the theory of *trains-loops-tails.* The flexibility of the DNA molecule is quantified by the “persistence length” and describes the length within the DNA molecule without conformational changes, which is ~50 nm (150bp) (Lu et al. 2001). Below the “persistence length” a DNA molecule behaves as a stiff rod, because of repulsion between the negatively charged phosphate groups in the DNA backbone (Lu et al. 2001; Singh et al. 2025). Stiffness of polyelectrolytes also depends on ionic strength and valency of cations. In this thesis, no conformational changes due to varying ionic strength are expected, as the salt concentration and cations are same over all experiments. Transferring that to the results of this thesis, 99 bp DNA adsorbs flat on the surface of the mineral, while 1000 bp DNA and gDNA adsorb just partly and build structures of flexible *tails* and *loops* (chapter 1.4.2). Singh et al. 2025 hypothesizes that the adsorption of short DNA fragments as stiff rods, leads to an increased surface footprint, as they are occupying more surface area per molecule compared to longer, flexible DNA fragments. Furthermore, the adsorption of DNA to the goethite surface leads to an increasingly negative bulk charge (charge overcompensation) and thus to electrostatic repulsion between short DNA-mineral associations and hence increasingly dispersed DNA-goethite conjugates (Skalny et al. 2024). Long DNA fragments on the other hand extend between particles, leading to mineral particle bridging and flocculation (Gregory und Barany 2011; Skalny et al. 2024; Singh et al. 2025). Both, higher surface footprint in relation to polymer length of short DNA fragments and the inhibition of DNA adsorption due to charge overcompensation leads to an overall lower DNA mass adsorption of shorter DNA fragments compared to longer DNA fragments (Singh et al. 2025).

Longer DNA polymers adsorb more compared to shorter ones, as they counteract charge overcompensation through mineral particle bridging and have a reduced surface footprint per molecule due to their *trains-loops-tails* adsorption architecture.

6.1.1 Effect of phosphate on DNA adsorption

The results of this study aligns with previous studies (Cai et al. 2007; Zhong et al. 2007; Sodnikar et al. 2021; Feng et al. 2024) and demonstrate, that DNA adsorption may be hindered by orthophosphate anions, as they compete for the same adsorption sites The data presented in Figure 5 show reduced adsorption at 1 mM phosphate compared to 0.1 mM phosphate, indicating strong competition of phosphate with DNA at higher concentrations. Phosphate does not just compete with DNA for adsorption sites, to block DNA (Chen et al. 2025), but also lowers the charge of the goethite surface (Szewczuk-Karpisz et al. 2023), which decreases DNA adsorption due to electrostatic repulsion. This results align well with the findings of previous studies (Cai et al. 2007; Feng et al. 2024).

The order of addition experiments with phosphate presented in Figure 5 show, that DNA adsorption kinetics, converge at higher phosphate concentration, indicating that thermodynamic equilibrium is reached at strongly competitive conditions. In contrast, at low phosphate concentration, adsorption and desorption kinetics do not converge and remain kinetically controlled. This indicates that the ability of the system to reach thermodynamic equilibrium depends on phosphate concentration.

Additionally, phosphate-induced DNA desorption strongly depends on DNA polymer length decreasing in the order 99 bp>1000 bp>gDNA. This trend remains consistent across all tested phosphate concentrations (Fig. 5 and 7). These findings align with recent results from Chen et al. 2025, who reported that the efficiency of phosphate-induced DNA desorption is inversely proportional to the length of linear DNA fragments. This can be attributed to the length-dependent number of Fe–O–P bonds between phosphate groups of the DNA backbone and surface hydroxyl groups on goethite. Longer DNA polymers establish substantially more Fe–O–P bonds per molecule, which increases the energetic barrier for desorption (Feng et al. 2024; Chen et al. 2025). Consequently, the displacement of these bonds during phosphate-induced DNA desorption is more efficient for shorter DNA molecules, resulting in higher desorption rates, as the probability of simultaneous displacement of all bonds by phosphate increases (Chen et al. 2025).

The results of the DNA adsorption experiment with subsequent addition of phosphate (Fig. 7) show furthermore, that DNA desorption increases with increasing phosphate concentration. Higher phosphate concentrations lead to more efficient competition between DNA and orthophosphate (Chen et al. 2025). However, there is a residual fraction of DNA that does not desorb at 100 mM phosphate even though goethite surface is overs-saturated already at 5mM phosphate, as shown in the phosphate adsorption isotherm (Fig. 4C). It has been reported about

residual, “irreversibly bound” DNA fractions on Fe(III)-(oxyhydr)oxides recently (Hettiarachchi and Grassian 2024; Chen et al. 2025). Note that Hettiarachchi and Grassian 2024 used pH 5, which favours DNA adsorption to goethite. This residual fraction of adsorbed DNA is attributed to the formation of covalent Fe-O-P bonds, that enhances DNA adsorption at high pH and may lead to irreversibly adsorbed DNA (Mauvisseau et al. 2022). Feng et al. 2024 directly compared the binding strength of nucleic acids and orthophosphate to goethite and showed that, as the number of phosphate groups participating in Fe–O–P bonding per DNA molecule increases, the likelihood of simultaneous desorption of all bonds decreases. This might explain the polymer-length-dependent residual DNA fraction that remains irreversibly bound to goethite even at very high phosphate concentrations. This residual DNA fraction may increase the plateau of the desorption kinetics. The longer time required to reach the plateau during desorption, compared to adsorption can be explained by multiple Fe-O-P bonds of DNA polymers, that requires simultaneous breaking by phosphate anions, which is statistically less likely in shorter time and therefore a slower process (Singh et al. 2025), whereas adsorption requires only few attachment points to be formed. This may lead to a metastable non-equilibrium state (Sukhishvili und Granick 1998), which is increasingly pronounced for longer DNA polymers and suggests kinetical trapping.

Adsorption of DNA under the influence of inorganic phosphate is controlled by polymer length, which results mainly from the ability of longer DNA polymers to form more Fe-O-P bonds per molecule. Furthermore, adsorption and desorption kinetics strongly depend on phosphate concentration, because of strong competition between phosphate-anions and DNA. The “irreversibly bound” DNA fraction and the comparatively slower DNA desorption indicate that phosphate induced desorption reaches a kinetically trapped state, rather than remaining kinetically controlled. Kinetical trapping is more pronounced for longer DNA polymers.

6.1.2 Effect of BSA on DNA adsorption

The results of this thesis shown in Figures 6 and 11 demonstrate full adsorption of longer DNA polymers on goethite with preadsorbed BSA, while the adsorption of shorter DNA polymers is hindered by high BSA concentrations. This might be due to the adsorption behaviour of BSA on goethite surface. OM does not distribute evenly across the mineral surface upon adsorption but instead forms localized clusters and discrete patches (Kleber et al. 2007). Previous studies have shown that BSA adsorbs to goethite with a heterogenous surface distribution (Kim und Grassian 2023), while others highlight the fact that proteins like BSA form aggregates in solution and adsorb as aggregated supramolecular structures (Rabe et al. 2011; Schmidt und Martínez 2018). The heterogenous surface of goethite with preadsorbed BSA may hinder the adsorption of stiff,

rod-shaped short DNA, while long, flexible DNA polymers may be able to reach exposed surface patches, forming Fe-O-P bonds. The work of Schmidt and Martínez 2018 on supramolecular associations of DNA and BSA in solution indicates that DNA may be able to adsorb onto preadsorbed BSA through a bridging mechanism in which BSA links DNA and goethite. However, based on given experimental conditions one would expect BSA-DNA repulsion, as both possess overall negative charge. It is suggested that local binding of positively charged side chain groups of BSA (e.g. lysine, arginine) to DNA, was one of the primary nonspecific interactions between proteins and nucleic acids (Hippel 2007; Schmidt und Martínez 2018) and may explain bridging at neutral pH. It has been found that BSA itself exhibits a heterogeneous surface charge distribution with localized positively charged patches, that enables interactions with polyelectrolytes, despite net charges would predict repulsion (Mattison et al. 1998). The heterogenous distribution of DNA-binding sites on preadsorbed BSA may again favour the adsorption of longer DNA polymers, as they can simultaneously interact with multiple positively charged side chains.

The BSA adsorption isotherm as well as BSA adsorption kinetics (Fig. 4 and 10) indicate strong affinity of BSA to goethite, which correlates well with previous studies (Tian et al. 2020). However, BSA cannot exchange preadsorbed DNA from goethite surface, as shown in Figure 6. Preadsorbed BSA on goethite hinders the adsorption of short “stiff” DNA fragments due to the patchy, heterogenous charge distribution on the goethite surface and BSA itself. In contrast, longer “flexible” DNA polymers can bridge these patches and thus adsorb to both, the goethite surface and surface-bound BSA, such that total DNA adsorption is not reduced.

6.2 Effect of polymer length and competing species on the enzymatic degradation of DNA on goethite

Overall, the results suggest that enzymatic hydrolysis of DNA is strongly governed by the presence of competing species and the DNA polymer length (Fig. 8 and 9). Degradation of adsorbed DNA increases with polymer length in the order 99 bp<1000 bp<gDNA. Hesslink`s model of polyelectrolyte adsorption that describes how charged polymers adsorb as *trains-loops-tails* serves, to explain the experimental results. While shorter DNA polymers adsorb as stiff rod-shaped molecules flat on the goethite surface as so-called *trains*, longer DNA polymers adsorb with interspersed surface-bound segments (*trains*), with substantial parts of their long flexible strands forming *loops* and *tails* that extend freely into the solvent (Jenckel and Rumbach 1951; Hesselink 1977; Sodnikar et al. 2021). These solvent-exposed parts of long DNA polymers are therefore not protected through adsorption and prone to enzymatic hydrolysis. Control

batches of the degradation experiments without mineral show that DNA in solution is degraded completely by enzymatic hydrolysis within experimental conditions. That is in line with the findings of Brundin et al. 2013 who showed, that DNA in solution is completely degraded within 30 minutes. The electropherogram (Fig. 8D) of the 99 bp DNA degradation experiment shows that a fraction of adsorbed 99 bp DNA retains its original polymer length after enzymatic hydrolysis, indicating that parts of the DNA is not fragmented by DNase I and therefore protected. At the same time, a substantial fraction of the 99 bp DNA is degraded into shorter fragments. These <99 bp fragments are detectable only in samples without phosphate and at low phosphate concentration. This <99 bp DNA fraction may arise from DNA that is degraded at their solvent-exposed *tails* and *loops*, which is unlikely for 99 bp DNA as it is assumed that 99 bp DNA adsorbs flat on the surface. Moreover, the <99 bp DNA fragments indicate, that DNase I also attacks parts of DNA, which are adsorbed flat as *trains*. Based on the data for 1000 bp and gDNA experiments it remains uncertain if the peak at 100 bp depicts degradation products or if this is the fraction of adsorbed DNA considered as *trains* that never experienced direct enzymatic attack. Since small DNA fragments preferentially adsorb in competition with longer DNA polymers (Singh et al. 2025), degradation products likely explain the peak at ~100 bp, rather than non-degraded *trains*.

The results of the degradation experiments offer further evidence that DNA exposed to degradation leads to highly fragmented DNA polymers with preferential preservation of fragments at 100 bp or smaller (Pääbo 1989; Deagle et al. 2006; Pietramellara et al. 2009; Dabney et al. 2013). Furthermore, it was proved that mineral-associated DNA is partly protected from enzymatic hydrolysis, while the protection effect depends on DNA polymer length.

6.2.1 Effect of phosphate on enzymatic degradation

The results of the degradation experiments under the influence of preadsorbed phosphate (Fig. 8A-C) show that the degradation of mineral-associated DNA increases with increasing phosphate concentration. As discussed previously, preadsorbed phosphate decreases DNA adsorption by blocking binding sites and lowering the surface charge of goethite. Therefore, more DNA remains in solution, where it gets easily degraded by DNase I. At 0.1 mM phosphate most of the gDNA is adsorbed, still there is no DNA surviving. This can be attributed to the fact that long DNA polymers (e.g. gDNA), are more susceptible to degradation. However, a second protection mechanism may play a role there. Previous works highlighted the fact, that DNA protection against enzymatic degradation is not solely governed by DNA adsorption but also through the physical separation of DNA from DNase I, as the nuclease adsorbs to mineral surface too (Demanèche et al. 2001; Cai et al. 2006b; Brundin et al. 2013). Increasing surface-bound

phosphate is expected to reduce DNase I adsorption and consequently, to decrease enzyme inactivation by surface binding.

The experimental results suggest two effects of increasing phosphate concentrations on enzymatic degradation of mineral-associated DNA: First, the competition of phosphate with DNA reduces DNA adsorption and consequently makes it more available for degradation. Second, increasing phosphate concentration decreases DNase I adsorption to the mineral surface and thus increases the concentration of active enzyme in solution. While the first argument was proved experimentally, the second argument about DNase I adsorption needs to be addressed in further experiments.

6.2.2 Effect of BSA on enzymatic degradation

The degradation experiments with preadsorbed BSA show that the fraction of the initially adsorbed DNA that degrades through enzymatic hydrolysis increases with increasing BSA concentration for 1000 bp and gDNA (Fig. 9B, C). While the fraction of the 99 bp DNA degradation products (Fig. 9A) remains stable. These results indicate that longer DNA polymers adsorbed onto BSA-associated goethite are more susceptible to enzymatic degradation. In addition to the *loops* and *tails* of longer DNA polymers, enzymatic activity may be increased by decreasing enzyme adsorption due to competition with BSA. Previous studies have shown that BSA blocks DNase I from adsorbing to illite, and therefore increases nuclease activity in solution (Demanèche et al. 2001), because BSA blocks binding sites for the DNase I enzyme. Therefore, DNase I remains available to degrade DNA preferentially at the solvent-exposed *loops* and *tails*. Furthermore, the peak shifts observed in Figure 9D and E indicate that increasingly smaller DNA fragments survive with increasing BSA concentration. Additionally, the right-skewness of the DNA size distribution after enzymatic hydrolysis decreases with increasing BSA concentration (Fig. 9D, E). Both supports the argument of more effective enzymatic hydrolysis with increasing BSA concentration.

However, the results of the degradation experiments with 99 bp shows an opposite trend, as DNA degradation with respect to initially adsorbed DNA remains stable with increasing BSA concentration. Additionally, the electropherogram (Fig. 9D) show that a fraction of the 99 bp DNA consistently retains its original fragment length after adding DNase I, regardless of the BSA concentration. Both indicates that DNA shorter than the “persistence length” adsorbs partly in a geometry that makes the polymer inaccessible for enzymatic hydrolysis. Assuming a heterogenous, patchy adsorption of BSA with clustering and the formation of multilayers (Kleber et al. 2007; Rabe et al. 2011; Schmidt und Martínez 2018; Barreto et al. 2020; Kim und Grassian 2023), fractions of the short DNA polymers may adsorb flat within the open surface patches and

the multilayer, where they would be physically protected, as BSA shields DNase I from the surface (Cai et al. 2006b).

These findings show that preadsorbed BSA on goethite increases DNA degradation, as it hinders DNA and DNase I adsorption. This is counteracted for 99 bp DNA polymers, probably because short DNA fragments are physically protected by BSA clusters. This provides further evidence for the predominance of highly fragmented eDNA.

7 Conclusion

This thesis investigates the impact of competing species (BSA and phosphate) and DNA polymer length (99 bp DNA, 1000 bp DNA and gDNA) on adsorption and enzymatic hydrolysis of DNA on goethite. The results show that irrespective of the presence, type and concentration of competing species, DNA adsorption increases with polymer length due to the prevailing adsorption as *loops* and *tails* for longer DNA molecule and therefore a reduced foodprint per molecule. This suggests that longer DNA polymers show a higher adsorption capacity to minerals in the environment. Desorption of DNA in the presence of inorganic phosphate also depends on polymer length, as longer DNA molecules can form a larger number of Fe–O–P bonds per molecule, which requires simultaneous breaking of these bonds. As equilibrium cannot be attained within 504 hours DNA adsorption-desorption processes under the influence of phosphate are kinetically controlled. However, the persistence of an “irreversibly bound” DNA fraction and the comparatively slow phosphate induced DNA desorption rate indicate that DNA-phosphate competition leads to kinetically trapped, metastable states rather than purely kinetically controlled processes. This kinetical trapping becomes increasingly pronounced with increasing DNA polymer length, reflecting the larger number of phosphate groups involved in surface bonding and the resulting higher degree of metastability. As shown by previous studies, this thesis confirms that phosphate is a strong competitor of DNA due to similar adsorption mechanism of DNA and phosphate on goethite. Phosphate reduces the adsorption of DNA onto goethite by inhibiting adsorption as well as desorbing DNA. The extent of this competition is influenced by both the concentration of phosphate and DNA polymer length. BSA on the other hand couldn’t desorb preadsorbed DNA even at high concentrations. The presence of BSA on goethite surface mainly affected the adsorption of shorter DNA polymers due to the patchy, heterogenous charge distribution on the BSA-mineral surface, while longer “flexible” DNA polymers may bridge these patches. It was experimentally confirmed that enzymatic hydrolysis of DNA adsorbed to goethite leads to highly fragmented DNA with a preferential preservation of 100 bp or smaller. DNA degradation increases with DNA polymer length, as longer DNA

polymers exhibit large parts of solvent exposed *tails* and *loops.* The presence of BSA and phosphate on the surface of goethite, resulted in more degradation compared to pristine goethite, as they reduce DNA adsorption. Additionally, DNase I adsorption may be partly blocked by competing species, making the enzyme more available and enhance DNA degradation. Furthermore, the results of the 99 bp DNA degradation experiments with preadsorbed BSA indicate, that *trains* of short DNA polymers may be incorporated within the BSA multilayer on the goethite surface leading to physical protection against enzymatic hydrolysis.

To assess the environmental implications of phosphate on DNA adsorption and degradation, it is necessary, to constrain interpretations to environmentally relevant concentrations. In this case phosphate ranges between 0.0001 – 0.26 mM, but usually below 0.01 mM (Mulqueen et al. 2004; Ducousso-Détrez et al. 2022). Therefore, gDNA adsorption would not be substantially affected by environmentally relevant phosphate concentrations, while short DNA fragments are already prone to desorption. However, short DNA fragments at 0.01 mM phosphate are protected better against enzymatic hydrolysis than longer DNA polymers. These results suggest, that for choosing sampling sites for eDNA/aDNA e.g. cave sediments, potential phosphate enrichment due to guano deposits (de-Dios et al. 2025; Gelabert et al. 2025) or bone dissolution (Biswas et al. 2022) should be considered. Also, the strong competition between DNA and phosphate indicates that elevated phosphate concentrations, for example in heavily fertilized soils, must be considered when evaluating the environmental fate of double-stranded RNA (dsRNA) from genetically modified RNA interference (RNAi) crops in agricultural systems (Sodnikar et al. 2021).

This work demonstrates that long-term DNA preservation is promoted by adsorption onto goethite surfaces at low phosphate concentrations, as well as by interactions with OM associated with the mineral surface. DNA polymers smaller than 100 bp were particularly protected against enzymatic hydrolysis, which may be supported by the incorporation into OM structures on the mineral surface.

Future research should further investigate the structure of OM adsorbed onto mineral surfaces and its potential to protect DNA from enzymatic degradation. In addition, future studies on enzymatic hydrolysis of DNA polymers should consider the influence of competing ions and organic matter on DNase I activity, particularly potential competitive effects during DNA degradation. Moreover, the presence of divalent cations in the environment may also affect DNA–goethite interactions, as well as competitive processes and degradation dynamics and therefore requires further investigation.

9 Bibliography

Alaeddini, Reza; Walsh, Simon J.; Abbas, Ali (2010): Forensic implications of genetic analyses from degraded DNA--a review. In: *Forensic science international. Genetics* 4 (3), S. 148–157. DOI: 10.1016/j.fsigen.2009.09.007.

Allwood, Julia S.; Fierer, Noah; Dunn, Robert R. (2020): The Future of Environmental DNA in Forensic Science. In: *Applied and environmental microbiology* 86 (2). DOI: 10.1128/AEM.01504-19.

Antelo, Juan; Avena, Marcelo; Fiol, Sarah; López, Rocío; Arce, Florencio (2005): Effects of pH and ionic strength on the adsorption of phosphate and arsenate at the goethite-water interface. In: *Journal of Colloid and Interface Science* 285 (2), S. 476–486. DOI: 10.1016/j.jcis.2004.12.032.

Balsam, William L.; Otto-Bliesner, Bette L.; Deaton, Bobby C. (1995): Modern and Last Glacial Maximum eolian sedimentation patterns in the Atlantic Ocean interpreted from sediment iron oxide content. In: *Paleoceanography* 10 (3), S. 493–507. DOI: 10.1029/95PA00421.

Barreto, Matheus Sampaio C.; Elzinga, Evert J.; Alleoni, Luís Reynaldo F. (2020): The molecular insights into protein adsorption on hematite surface disclosed by in-situ ATR-FTIR/2D-COS study. In: *Sci Rep* 10 (1), S. 13441. DOI: 10.1038/s41598-020-70201-z.

Barrón, Vidal; Torrent, José (2013): Iron, manganese and aluminium oxides and oxyhydroxides. DOI: 10.1180/EMU-notes.14.9

Benndorf, Dirk; Balcke, Gerd U.; Harms, Hauke; Bergen, Martin von (2007): Functional metaproteome analysis of protein extracts from contaminated soil and groundwater. In: *The ISME journal* 1 (3), S. 224–234. DOI: 10.1038/ismej.2007.39.

Biswas, Partha Pratim; Turner-Walker, Gordon; Rathod, Jagat; Liang, Biqing; Wang, Chun-Chieh; Lee, Yao-Chang; Sheu, Hwo-Shuenn (2022): Sustainable phosphorus management in soil using bone apatite. In: *Journal of environmental management* 305, S. 114344. DOI: 10.1016/j.jenvman.2021.114344.

Blum, Stephanie A.E.; Lorenz, Michael G.; Wackernagel, Wilfried (1997): Mechanism of Retarded DNA Degradation and Prokaryotic Origin of DNases in Nonsterile Soils. In: *Systematic and Applied Microbiology* 20 (4), S. 513–521. DOI: 10.1016/S0723-2020(97)80021-5.

Brundin, Malin; Figdor, David; Sundqvist, Göran; Sjögren, Ulf (2013): DNA binding to hydroxyapatite: a potential mechanism for preservation of microbial DNA. In: *Journal of Endodontics* 39 (2), S. 211–216. DOI: 10.1016/j.joen.2012.09.013.

Cai, P.; Huang, Q.; Zhang, X.; Chen, H. (2006a): Adsorption of DNA on clay minerals and various colloidal particles from an Alfisol. In: *Soil Biology and Biochemistry* 38 (3), S. 471–476. DOI: 10.1016/j.soilbio.2005.05.019.

Cai, Peng; Huang, Qiaoyun; Zhu, Jun; Jiang, Daihua; Zhou, Xueyong; Rong, Xingmin; Liang, Wei (2007): Effects of low-molecular-weight organic ligands and phosphate on DNA adsorption by soil colloids and minerals. In: *Colloids and Surfaces B: Biointerfaces* 54 (1), S. 53–59. DOI: 10.1016/j.colsurfb.2006.07.013.

Cai, Peng; Huang, Qiao-Yun; Zhang, Xue-Wen (2006b): Interactions of DNA with clay minerals and soil colloidal particles and protection against degradation by DNase. In: *Environmental science & technology* 40 (9), S. 2971–2976. DOI: 10.1021/es0522985.

Chen, Zaiming; Wang, Tianzhu; Zhang, Kaiyi; Cheng, Jiajun; Wang, Meizhen (2025): Goethite nanoparticles binding DNA in dissemination of antibiotic resistance genes: new insights into the role of inorganic phosphate with environmentally relevant concentrations. In: *Environ. Sci.: Nano* 12 (11), S. 5036–5047. DOI: 10.1039/D5EN00765H.

Chourey, Karuna; Jansson, Janet; VerBerkmoes, Nathan; Shah, Manesh; Chavarria, Krystle L.; Tom, Lauren M. et al. (2010): Direct cellular lysis/protein extraction protocol for soil metaproteomics. In: *Journal of proteome research* 9 (12), S. 6615–6622. DOI: 10.1021/pr100787q.

Cornell, Rochelle M.; Schwertmann, Udo (2006): The iron oxides. Structure, properties, reactions, occurrences and uses. 2., compl. rev. and extended ed., repr. Weinheim: Wiley-VCH.

Crecchio, C.; Stotzky, G. (1998): Binding of DNA on humic acids: Effect on transformation of Bacillus subtilis and resistance to DNase. In: *Soil Biology and Biochemistry* 30 (8-9), S. 1061–1067. DOI: 10.1016/S0038-0717(97)00248-4.

Dabney, Jesse; Meyer, Matthias; Pääbo, Svante (2013): Ancient DNA damage. In: *Cold Spring Harbor perspectives in biology* 5 (7). DOI: 10.1101/cshperspect.a012567.

Dai, Guohua; Zhu, Shanshan; Cai, Yue; Zhu, Erxiong; Jia, Yufu; Ji, Chengjun et al. (2022): Plant-derived lipids play a crucial role in forest soil carbon accumulation. In: *Soil Biology and Biochemistry* 168, S. 108645. DOI: 10.1016/j.soilbio.2022.108645.

Das, Soumya; Hendry, M. Jim (2011): Changes of crystal morphology of aged goethite over a range of pH (2–13) at 100°C. In: *Applied Clay Science* 51 (1-2), S. 192–197. DOI: 10.1016/j.clay.2010.11.006.

Deagle, Bruce E.; Eveson, J. Paige; Jarman, Simon N. (2006): Quantification of damage in DNA recovered from highly degraded samples--a case study on DNA in faeces. In: *Front Zool* 3 (1), S. 11. DOI: 10.1186/1742-9994-3-11.

de-Dios, Toni; Bonucci, Biancamaria; Barbieri, Rémi; Kushniarevich, Alena; D'Atanasio, Eugenia; Dittmar, Jenna et al. (2025): Bone Adhered Sediments as a Source of Target and Environmental DNA and Proteins. In: *Molecular Biology and Evolution* 42 (9), msaf202. DOI: 10.1093/molbev/msaf202.

Dell'Anno, Antonio; Corinaldesi, Cinzia (2004): Degradation and turnover of extracellular DNA in marine sediments: ecological and methodological considerations. In: *Applied and environmental microbiology* 70 (7), S. 4384–4386. DOI: 10.1128/AEM.70.7.4384-4386.2004.

Demanèche, S.; Jocteur-Monrozier, L.; Quiquampoix, H.; Simonet, P. (2001): Evaluation of biological and physical protection against nuclease degradation of clay-bound plasmid DNA. In: *Applied and environmental microbiology* 67 (1), S. 293–299. DOI: 10.1128/AEM.67.1.293-299.2001.

Dobrynin, Andrey V.; Rubinstein, Michael (2005): Theory of polyelectrolytes in solutions and at surfaces. In: *Progress in Polymer Science* 30 (11), S. 1049–1118. DOI: 10.1016/j.progpolymsci.2005.07.006.

Ducousso-Détrez, Amandine; Fontaine, Joël; Lounès-Hadj Sahraoui, Anissa; Hijri, Mohamed (2022): Diversity of Phosphate Chemical Forms in Soils and Their Contributions on Soil Microbial Community Structure Changes. In: *Microorganisms* 10 (3). DOI: 10.3390/microorganisms10030609.

Feng, Huajun; Ma, Shanshan; Chen, Zaiming; Li, Yungui; Wang, Meizhen; Ding, Yangcheng (2024): Adsorption of nucleotides and nucleic acids on goethite nanoparticles: mode, sites and relationship with phosphate and non-phosphate structures. In: *Environ. Sci.: Nano* 11 (6), S. 2655–2667. DOI: 10.1039/D3EN00891F.

Franchi, Marco; Ferris, James P.; Gallori, Enzo (2003): Cations as mediators of the adsorption of nucleic acids on clay surfaces in prebiotic environments. In: *Origins of life and evolution of the biosphere : the journal of the International Society for the Study of the Origin of Life* 33 (1), S. 1–16. DOI: 10.1023/a:1023982008714.

Frank-Kamenetskii, Maxim D. (1997): Biophysics of the DNA molecule. In: *Physics Reports* 288 (1-6), S. 13–60. DOI: 10.1016/S0370-1573(97)00020-3.

Frank-Kamenetskiĭ, M. D.; Anshelevich, V. V.; Lukashin, A. V. (1987): Polyelectrolyte model of DNA. In: *Sov. Phys. Usp.* 30 (4), S. 317–330. DOI: 10.1070/PU1987v030n04ABEH002833.

Gardner, Courtney M.; Gunsch, Claudia K. (2017): Adsorption capacity of multiple DNA sources to clay minerals and environmental soil matrices less than previously estimated. In: *Chemosphere* 175, S. 45–51. DOI: 10.1016/j.chemosphere.2017.02.030.

Gelabert, Pere; Oberreiter, Victoria; Straus, Lawrence Guy; Morales, Manuel Ramón González; Sawyer, Susanna; Marín-Arroyo, Ana B. et al. (2025): A sedimentary ancient DNA perspective on human and carnivore persistence through the Late Pleistocene in El Mirón Cave, Spain. In: *Nat Commun* 16 (1), S. 107. DOI: 10.1038/s41467-024-55740-7.

Gniazdowska, Agnieszka; Palinska-Saadi, Adriana; Krawczyk, Ewelina; Elzanowska, Hanna; Maj-Zurawska, Magdalena (2013): Supercoiled and linear plasmid DNAs interactions with methylene blue. In: *Bioelectrochemistry* 92, S. 32–41. DOI: 10.1016/j.bioelechem.2013.02.001.

Gregory, John; Barany, Sandor (2011): Adsorption and flocculation by polymers and polymer mixtures. In: *Advances in Colloid and Interface Science* 169 (1), S. 1–12. DOI: 10.1016/j.cis.2011.06.004.

Haas, Bruno; Bonifait, Laetitia; Vaillancourt, Katy; Charette, Steve J.; Gottschalk, Marcelo; Grenier, Daniel (2014): Characterization of DNase activity and gene in Streptococcus suis and evidence for a role as virulence factor. In: *BMC Res Notes* 7 (1), S. 424. DOI: 10.1186/1756-0500-7-424.

Häder, Donat-Peter; Kumar, H. D.; Smith, Ray C.; Worrest, Robert C. (2003): Aquatic ecosystems: effects of solar ultraviolet radiation and interactions with other climatic change factors. In: *Photochemical & photobiological sciences : Official journal of the European Photochemistry Association and the European Society for Photobiology* 2 (1), S. 39–50. DOI: 10.1039/B211160H.

Hesselink, F.Th (1977): On the theory of polyelectrolyte adsorption. In: *Journal of Colloid and Interface Science* 60 (3), S. 448–466. DOI: 10.1016/0021-9797(77)90309-5.

Hettiarachchi, Eshani; Grassian, Vicki H. (2024): Impact of Surface Adsorption on DNA Structure and Stability: Implications for Environmental DNA Interactions with Iron Oxide Surfaces. In: *Langmuir* 40 (52), S. 27194–27205. DOI: 10.1021/acs.langmuir.4c02501.

Hiemstra, T.; van Riemsdijk, W. H. (1996): A Surface Structural Approach to Ion Adsorption: The Charge Distribution (CD) Model. In: *Journal of Colloid and Interface Science* 179 (2), S. 488–508. DOI: 10.1006/jcis.1996.0242.

Hippel, Peter H. von (2007): From "simple" DNA-protein interactions to the macromolecular machines of gene expression. In: *Annual review of biophysics and biomolecular structure* 36, S. 79–105. DOI: 10.1146/annurev.biophys.34.040204.144521.

Hofreiter, M.; Serre, D.; Poinar, H. N.; Kuch, M.; Pääbo, S. (2001): Ancient DNA. In: *Nat Rev Genet* 2 (5), S. 353–359. DOI: 10.1038/35072071.

Ibrahim, Muhammad; Iqbal, Muhammad; Tang, Yu-Ting; Khan, Sardar; Guan, Dong-Xing; Li, Gang (2022): Phosphorus Mobilization in Plant–Soil Environments and Inspired Strategies for Managing Phosphorus: A Review. In: *Agronomy* 12 (10), S. 2539. DOI: 10.3390/agronomy12102539.

Jenckel, E.; Rumbach, B. (1951): Über die Adsorption von hochmolekularen Stoffen aus der Lösung. In: *Zeitschrift für Elektrochemie und angewandte physikalische Chemie* 55 (7), S. 612–618. DOI: 10.1002/bbpc.19510550706.

Jiang, Zhaoxia; Liu, Qingsong; Dekkers, Mark J.; Barrón, Vidal; Torrent, José; Roberts, Andrew P. (2016): Control of Earth-like magnetic fields on the transformation of ferrihydrite to hematite and goethite. In: *Sci Rep* 6 (1), S. 30395. DOI: 10.1038/srep30395.

Jo, Toshiaki S. (2026): pH-Dependent Degradation of Macrobial Environmental DNA in Water. In: *Molecular ecology resources* 26 (2), e70101. DOI: 10.1111/1755-0998.70101.

Kasyanenko, Nina; Khansetsen, Bolorkhuu; Baryshev, Andrey; Sokolov, Petr (2025): DNA Persistent Length in Solutions of Different pH. In: *International journal of molecular sciences* 27 (1). DOI: 10.3390/ijms27010316.

Kim, Deborah; Grassian, Vicki H. (2023): Analysis of micro- and nanoscale heterogeneities within environmentally relevant thin films containing biological components, oxyanions and minerals using AFM-PTIR spectroscopy. In: *Environ. Sci.: Processes Impacts* 25 (3), S. 484–495. DOI: 10.1039/d3em00005b.

Kim, Jongsik; Li, Wei; Philips, Brian L.; Grey, Clare P. (2011): Phosphate adsorption on the iron oxyhydroxides goethite (α-FeOOH), akaganeite (β-FeOOH), and lepidocrocite (γ-FeOOH): a 31P NMR Study. In: *Energy Environ. Sci.* 4 (10), S. 4298. DOI: 10.1039/C1EE02093E.

Kjær, Kurt H.; Winther Pedersen, Mikkel; Sanctis, Bianca de; Cahsan, Binia de; Korneliussen, Thorfinn S.; Michelsen, Christian S. et al. (2022): A 2-million-year-old ecosystem in Greenland uncovered by environmental DNA. In: *Nature* 612 (7939), S. 283–291. DOI: 10.1038/s41586-022-05453-y.

Kleber, M.; Sollins, P.; Sutton, R. (2007): A conceptual model of organo-mineral interactions in soils: self-assembly of organic molecular fragments into zonal structures on mineral surfaces. In: *Biogeochemistry* 85 (1), S. 9–24. DOI: 10.1007/s10533-007-9103-5.

Levy-Booth, David J.; Campbell, Rachel G.; Gulden, Robert H.; Hart, Miranda M.; Powell, Jeff R.; Klironomos, John N. et al. (2007): Cycling of extracellular DNA in the soil environment. In: *Soil Biology and Biochemistry* 39 (12), S. 2977–2991. DOI: 10.1016/j.soilbio.2007.06.020.

Lindahl, T. (1993): Instability and decay of the primary structure of DNA. In: *Nature* 362 (6422), S. 709–715. DOI: 10.1038/362709a0.

Liu, Jing; Zhu, Runliang; Ma, Lingya; Fu, Haoyang; Lin, Xiaoju; Parker, Stephen C.; Molinari, Marco (2021): Adsorption of phosphate and cadmium on iron (oxyhydr)oxides: A comparative study on ferrihydrite, goethite, and hematite. In: *Geoderma* 383, S. 114799. DOI: 10.1016/j.geoderma.2020.114799.

Liu, Yun; Sheng, Xia; Dong, Yuanhua; Ma, Yijie (2012): Removal of high-concentration phosphate by calcite: Effect of sulfate and pH. In: *Desalination* 289, S. 66–71. DOI: 10.1016/j.desal.2012.01.011.

Lorenz, M. G.; Wackernagel, W. (1987): Adsorption of DNA to sand and variable degradation rates of adsorbed DNA. In: *Applied and environmental microbiology* 53 (12), S. 2948–2952. DOI: 10.1128/aem.53.12.2948-2952.1987.

Lorenz, M. G.; Wackernagel, W. (1994): Bacterial gene transfer by natural genetic transformation in the environment. In: *Microbiological reviews* 58 (3), S. 563–602. DOI: 10.1128/mr.58.3.563-602.1994.

Lu, Y.; Weers, B.; Stellwagen, N. C. (2001): DNA persistence length revisited. In: *Biopolymers* 61 (4), S. 261–275. DOI: 10.1002/bip.10151.

Mattison, Kevin W.; Dubin, Paul L.; Brittain, Isabelle J. (1998): Complex Formation between Bovine Serum Albumin and Strong Polyelectrolytes: Effect of Polymer Charge Density. In: *J. Phys. Chem. B* 102 (19), S. 3830–3836. DOI: 10.1021/jp980486u.

Mauvisseau, Quentin; Harper, Lynsey R.; Sander, Michael; Hanner, Robert H.; Kleyer, Hannah; Deiner, Kristy (2022): The Multiple States of Environmental DNA and What Is Known about Their Persistence in Aquatic Environments. In: *Environmental science & technology* 56 (9), S. 5322–5333. DOI: 10.1021/acs.est.1c07638.

Messina, René; Holm, Christian; Kremer, Kurt (2004): Polyelectrolyte adsorption and multilayering on charged colloidal particles. In: *J Polym Sci B Polym Phys* 42 (19), S. 3557–3570. DOI: 10.1002/polb.20203.

Mikutta, Robert; Mikutta, Christian; Kalbitz, Karsten; Scheel, Thorsten; Kaiser, Klaus; Jahn, Reinhold (2007): Biodegradation of forest floor organic matter bound to minerals via different binding mechanisms. In: *Geochimica et Cosmochimica Acta* 71 (10), S. 2569–2590. DOI: 10.1016/j.gca.2007.03.002.

Mulqueen, J.; Rodgers, M.; Scally, P. (2004): Phosphorus transfer from soil to surface waters. In: *Agricultural Water Management* 68 (1), S. 91–105. DOI: 10.1016/j.agwat.2004.10.006.

Murphy, J.; Riley, J. P. (1962): A modified single solution method for the determination of phosphate in natural waters. In: *Analytica Chimica Acta* 27, S. 31–36. DOI: 10.1016/S0003-2670(00)88444-5.

Nguyen, Thanh H.; Chen, Kai Loon (2007): Role of divalent cations in plasmid DNA adsorption to natural organic matter-coated silica surface. In: *Environmental science & technology* 41 (15), S. 5370–5375. DOI: 10.1021/es070425m.

Nielsen, Kaare M.; Johnsen, Pål J.; Bensasson, Douda; Daffonchio, Daniele (2007): Release and persistence of extracellular DNA in the environment. In: *Environmental biosafety research* 6 (1-2), S. 37–53. DOI: 10.1051/ebr:2007031.

Omoike, Anselm; Chorover, Jon; Kwon, Kideok D.; Kubicki, James D. (2004): Adhesion of bacterial exopolymers to alpha-FeOOH: inner-sphere complexation of phosphodiester groups. In: *Langmuir : the ACS journal of surfaces and colloids* 20 (25), S. 11108–11114. DOI: 10.1021/la048597.

Orlando, Ludovic; Allaby, Robin; Skoglund, Pontus; Der Sarkissian, Clio; Stockhammer, Philipp W.; Ávila-Arcos, María C. et al. (2021): Ancient DNA analysis. In: *Nat Rev Methods Primers* 1 (1). DOI: 10.1038/s43586-020-00011-0.

Pääbo, S. (1989): Ancient DNA: extraction, characterization, molecular cloning, and enzymatic amplification. In: *Proceedings of the National Academy of Sciences of the United States of America* 86 (6), S. 1939–1943. DOI: 10.1073/pnas.86.6.1939.

Parducci, Laura; Matetovici, Irina; Fontana, Sonia L.; Bennett, K. D.; Suyama, Yoshihisa; Haile, James et al. (2013): Molecular- and pollen-based vegetation analysis in lake sediments from central Scandinavia. In: *Molecular Ecology* 22 (13), S. 3511–3524. DOI: 10.1111/mec.12298.

Parsiegla, Goetz; Noguere, Christophe; Santell, Lydia; Lazarus, Robert A.; Bourne, Yves (2012): The structure of human DNase I bound to magnesium and phosphate ions points to a catalytic mechanism common to members of the DNase I-like superfamily. In: *Biochemistry* 51 (51), S. 10250–10258. DOI: 10.1021/bi300873f.

Pedersen, Mikkel Winther; Overballe-Petersen, Søren; Ermini, Luca; Sarkissian, Clio Der; Haile, James; Hellstrom, Micaela et al. (2015): Ancient and modern environmental DNA. In: *Philosophical transactions of the Royal Society of London. Series B, Biological sciences* 370 (1660), S. 20130383. DOI: 10.1098/rstb.2013.0383.

Pietramellara, G.; Ascher, J.; Borgogni, F.; Ceccherini, M. T.; Guerri, G.; Nannipieri, P. (2009): Extracellular DNA in soil and sediment: fate and ecological relevance. In: *Biol Fertil Soils* 45 (3), S. 219–235. DOI: 10.1007/s00374-008-0345-8.

Poly, Franck; Chenu, Claire; Simonet, Pascal; Rouiller, James; Jocteur Monrozier, Lucile (2000): Differences between Linear Chromosomal and Supercoiled Plasmid DNA in Their Mechanisms and Extent of Adsorption on Clay Minerals. In: *Langmuir* 16 (3), S. 1233–1238. DOI: 10.1021/la990506z.

Poté, John; Ackermann, Rafaël; Wildi, Walter (2009): Plant leaf mass loss and DNA release in freshwater sediments. In: *Ecotoxicology and Environmental Safety* 72 (5), S. 1378–1383. DOI: 10.1016/j.ecoenv.2009.04.010.

Pray, L. (2008): Discovery of DNA structure and function: Watson and Crick. In: *Nature Education* 1, Artikel 1, S. 100.

Rabe, Michael; Verdes, Dorinel; Seeger, Stefan (2011): Understanding protein adsorption phenomena at solid surfaces. In: *Advances in Colloid and Interface Science* 162 (1-2), S. 87–106. DOI: 10.1016/j.cis.2010.12.007.

Saeki, Kazutoshi; Kunito, Takashi; Sakai, Masao (2010): Effects of pH, ionic strength, and solutes on DNA adsorption by andosols. In: *Biol Fertil Soils* 46 (5), S. 531–535. DOI: 10.1007/s00374-010-0447-y.

Sand, Karina Krarup; Jelavić, Stanislav (2018): Mineral Facilitated Horizontal Gene Transfer: A New Principle for Evolution of Life? In: *Frontiers in microbiology* 9, S. 2217. DOI: 10.3389/fmicb.2018.02217.

Sawyer, Susanna; Krause, Johannes; Guschanski, Katerina; Savolainen, Vincent; Pääbo, Svante (2012): Temporal patterns of nucleotide misincorporations and DNA fragmentation in ancient DNA. In: *PloS one* 7 (3), e34131. DOI: 10.1371/journal.pone.0034131.

Scheinost, Andreas C.; Singh, Balwant (2023): Metal oxides. In: Michael Goßner und Margaret Oliver (Hg.): Encyclopedia of soils in the environment. Volume 1: Soil biology : Volume 2: Chemistry : Volume 3: Environment and management : Volume 4: Pedology, Pedometrics : Volume 5: Soil physics. Second edition. Amsterdam, Oxford, Cambridge: Elsevier, S. 135–148. Online verfügbar unter https://www.sciencedirect.com/science/article/pii/B9780128229743000690.

Schmidt, Michael P.; Martínez, Carmen E. (2017): Ironing Out Genes in the Environment: An Experimental Study of the DNA-Goethite Interface. In: *Langmuir : the ACS journal of surfaces and colloids* 33 (34), S. 8525–8532. DOI: 10.1021/acs.langmuir.7b01911.

Schmidt, Michael P.; Martínez, Carmen Enid (2018): Supramolecular Association Impacts Biomolecule Adsorption onto Goethite. In: *Environmental science & technology* 52 (7), S. 4079–4089. DOI: 10.1021/acs.est.7b06173.

Schulze, W. X. (2005): Protein analysis in dissolved organic matter: What proteins from organic debris, soil leachate and surface water can tell us - a perspective. In: *Biogeosciences* 2 (1), S. 75–86. DOI: 10.5194/bg-2-75-2005.

Schwertmann, Udo (2000): Iron oxides in the laboratory. Preparation and characterization. 2nd completely rev. and extended ed. Weinheim, New York: Wiley-VCH.

Sessions, S. K. (2013): Genome Size. In: Stanley Maloy, Kelly Hughes und Stanley R. Maloy (Hg.): Brenner's encyclopedia of genetics. 2nd ed. London: Academic Press Elsevier Science, S. 301–305. Online verfügbar unter https://www.sciencedirect.com/science/article/pii/B9780123749840006392.

Sharma, Pallavi; Jha, Ambuj Bhushan; Dubey, Rama Shanker; Pessarakli, Mohammad (2012): Reactive Oxygen Species, Oxidative Damage, and Antioxidative Defense Mechanism in Plants under Stressful Conditions. In: *Journal of Botany* 2012 (1), S. 1–26. DOI: 10.1155/2012/217037.

Singh, Veer Vikram; Kumar, Naresh; Kimber, Richard L.; Weiser, Ákos; Pinhasi, Ron; Kraemer, Stephan M. (2025): Polymer Length Governs DNA Adsorption Dynamics on Mineral Surfaces. In: *Environmental science & technology* 59 (38), S. 20462–20473. DOI: 10.1021/acs.est.5c08180.

Skalny, Mateusz; Rokowska, Anna; Szuwarzynski, Michal; Gajewska, Marta; Dziewit, Lukasz; Bajda, Tomasz (2024): Nanoscale surface defects of goethite governing DNA adsorption process and formation of the Goethite-DNA conjugates. In: *Chemosphere* 362, S. 142602. DOI: 10.1016/j.chemosphere.2024.142602.

Sodnikar, Katharina; Parker, Kimberly M.; Stump, Simona R.; ThomasArrigo, Laurel K.; Sander, Michael (2021): Adsorption of double-stranded ribonucleic acids (dsRNA) to iron (oxyhydr-)oxide surfaces: comparative analysis of model dsRNA molecules and deoxyribonucleic acids (DNA). In: *Environ. Sci.: Processes Impacts* 23 (4), S. 605–620. DOI: 10.1039/D1EM00010A.

Sommaruga, R. (2001): The role of solar UV radiation in the ecology of alpine lakes. In: *Journal of Photochemistry and Photobiology B: Biology* 62 (1-2), S. 35–42. DOI: 10.1016/S1011-1344(01)00154-3.

Strickler, Katherine M.; Fremier, Alexander K.; Goldberg, Caren S. (2015): Quantifying effects of UV-B, temperature, and pH on eDNA degradation in aquatic microcosms. In: *Biological Conservation* 183, S. 85–92. DOI: 10.1016/j.biocon.2014.11.038.

Stumm, Werner (1995): The Inner-Sphere Surface Complex. In: Chin P. Huang (Hg.): Aquatic chemistry. Interfacial and interspecies processes; developed from a Symposium sponsored by the Division of Environmental Chemistry, Inc. at the 203rd National Meeting of the American Chemical Society, San Francisco, California, April 5 - 10, 1992, Bd. 244. 2. pr. Washington, DC: American Chemical Society (National Meeting of the American Chemical Society, 203), S. 1–32.

Sukhishvili, Svetlana A.; Granick, Steve (1998): Kinetic regimes of polyelectrolyte exchange between the adsorbed state and free solution. In: *The Journal of Chemical Physics* 109 (16), S. 6869–6878. DOI: 10.1063/1.477254.

Szewczuk-Karpisz, Katarzyna; Kukowska, Sylwia; Grygorczuk-Płaneta, Katarzyna; Kondracki, Bartosz; Jerin, Katarina; Kovačević, Davor (2023): Scavenging of copper(II) ions, phosphate(V) ions, and diuron from aqueous media by goethite modified with chitosan or poly(acrylic acid). In: *Environ Sci Pollut Res* 30 (33), S. 79980–80000. DOI: 10.1007/s11356-023-27783-8.

Thomas, Christopher M.; Nielsen, Kaare M. (2005): Mechanisms of, and barriers to, horizontal gene transfer between bacteria. In: *Nature reviews. Microbiology* 3 (9), S. 711–721. DOI: 10.1038/nrmicro1234.

Tian, Zhaomo; Wang, Tao; Tunlid, Anders; Persson, Per (2020): Proteolysis of Iron Oxide-Associated Bovine Serum Albumin. In: *Environmental science & technology* 54 (8), S. 5121–5130. DOI: 10.1021/acs.est.0c00860.

Valko, M.; Rhodes, C. J.; Moncol, J.; Izakovic, M.; Mazur, M. (2006): Free radicals, metals and antioxidants in oxidative stress-induced cancer. In: *Chemico-biological interactions* 160 (1), S. 1–40. DOI: 10.1016/j.cbi.2005.12.009.

Verma, Taru; Hendiani, Saghar; Carbajo, Carlota; Andersen, Sandra B.; Hammarlund, Emma U.; Burmølle, Mette; Sand, Karina K. (2024): Recurrence and propagation of past functions through mineral facilitated horizontal gene transfer. In: *Frontiers in microbiology* 15, S. 1449094. DOI: 10.3389/fmicb.2024.1449094.

Whitmore, Liam; McCauley, Mark; Farrell, Jessica A.; Stammnitz, Maximilian R.; Koda, Samantha A.; Mashkour, Narges et al. (2023): Inadvertent human genomic bycatch and intentional capture raise beneficial applications and ethical concerns with environmental DNA. In: *Nat Ecol Evol* 7 (6), S. 873–888. DOI: 10.1038/s41559-023-02056-2.

Yagi, Shintaro; Fukushi, Keisuke (2012): Removal of phosphate from solution by adsorption and precipitation of calcium phosphate onto monohydrocalcite. In: *Journal of Colloid and Interface Science* 384 (1), S. 128–136. DOI: 10.1016/j.jcis.2012.06.063.

Ye, Mao; Zhang, Zhongyun; Sun, Mingming; Shi, Yu (2022): Dynamics, gene transfer, and ecological function of intracellular and extracellular DNA in environmental microbiome. In: *iMeta* 1 (3), e34. DOI: 10.1002/imt2.34.

Zhong, Bin; Stanforth, Robert; Wu, Shunnian; Chen, J. Paul (2007): Proton interaction in phosphate adsorption onto goethite. In: *Journal of Colloid and Interface Science* 308 (1), S. 40–48. DOI: 10.1016/j.jcis.2006.12.055.

8 Supplement Information (SI)

8.1 BSA adsorption kinetics

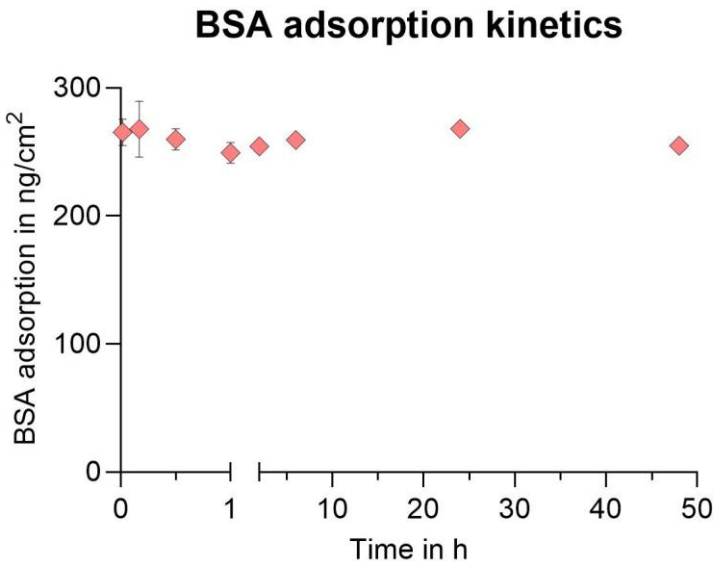

***Figure 10**: BSA adsorption kinetics; initial BSA concentration 300 ng/µl with sampling points ranging from 1-60 minutes up to 48 hours*

8.2 DNA adsorption as a function of preadsorbed BSA

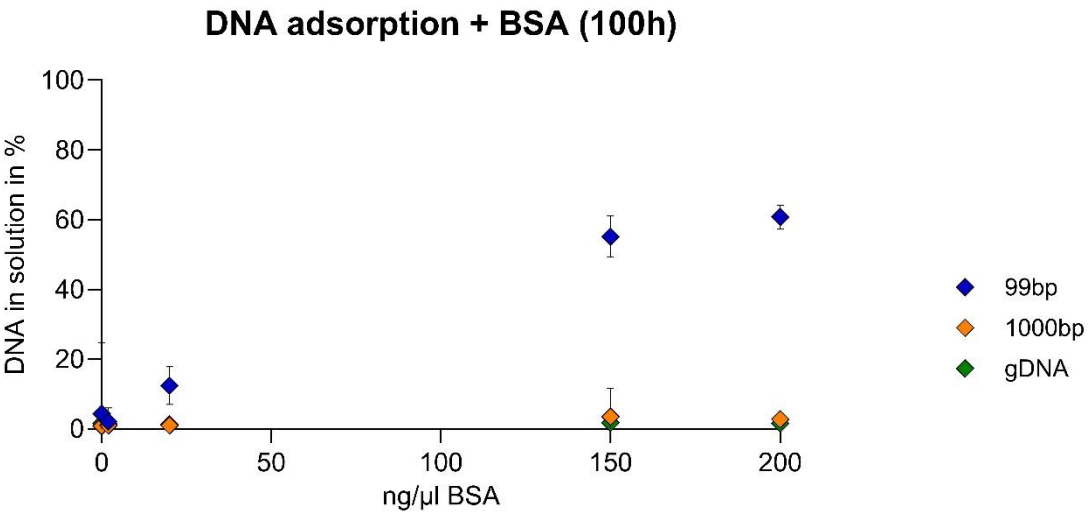

***Figure 11**: Adsorption of 40 ng/µl of 99 bp DNA, 1000 bp DNA and gDNA on goethite at BSA concentrations ranging from 0 and 200 ng/µl; DNA was preadsorbed for 18h followed by the adsorption of BSA for 100 h*

In Figure 11 DNA adsorption as a function of preadsorbed BSA was investigated. The longer DNA polymers (1000 bp and gDNA) are not affected of BSA being preadsorbed. Over the full BSA concentration, there is no DNA detectable in solution, which means full adsorption for 1000 bp and gDNA. In contrast, 99 bp DNA in solution rises with increasing BSA concentration up to 60%

DNA in solution. Therefore, 99 bp DNA adsorption decreases from 100% at 0 ng/µl BSA continuously to 40% adsorption with 200 ng/µl BSA

8.3 no DNase I control for gDNA

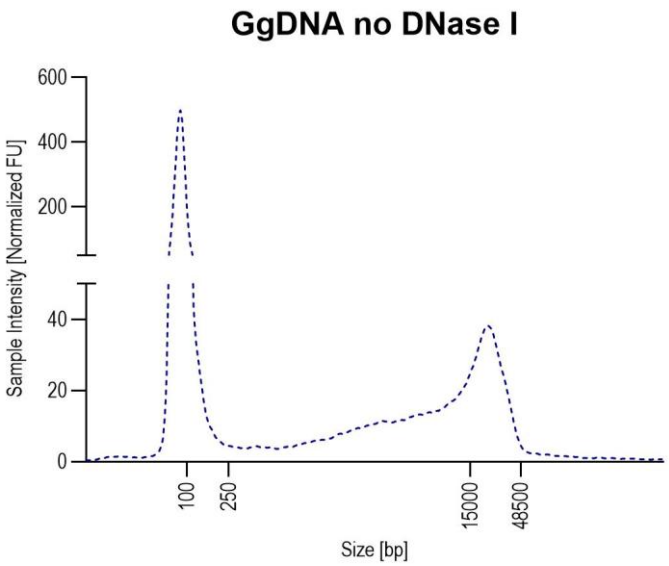

***Figure 12**: no DNase I control gDNA; Electropherogram of gDNA without DNase I*